

ALMA MATER STUDIORUM

UNIVERSITA' DI BOLOGNA

SCUOLA DI SCIENZE

Corso di laurea magistrale in BIOLOGIA MARINA

Inference of *Raja miraletus* population structure using mitochondrial and nuclear DNA: comparing the resolution power of molecular markers in exploring species and population boundaries.

Tesi di laurea in Struttura e connettività delle popolazioni marine

Relatrice

Dott.ssa Alessia Cariani

Presentata da

Alessia Crosara

Correlatori

Alice Ferrari

Fausto Tinti

III sessione

Anno Accademico 2014/2015

TABLE OF CONTENTS

1. INTRODUCTION	1
1.1. AIMS	6
2. MATERIALS AND METHODS	7
2.1. SAMPLING.....	7
2.2. DNA EXTRACTION & PCR AMPLIFICATION	8
2.2.1. Nuclear markers	8
2.2.2. Mitochondrial marker.....	9
2.3. DATA ANALYSIS	9
2.3.1. Nuclear markers dataset	9
2.3.2. Mitochondrial marker dataset assessment.....	9
2.3.3. Genetic diversity.....	10
2.3.4. Population differentiation.....	10
2.4. DEMOGRAPHIC HISTORY	11
3. RESULTS	12
3.1. Nuclear and mitochondrial markers dataset assessment	12
3.2. Genetic diversity.....	12
3.2.1. Nuclear markers polymorphism	12
3.2.2. Mitochondrial marker polymorphism	14
3.3. Population differentiation.....	15
3.4. Demographic history	29
4. DISCUSSION AND CONCLUSIONS	32
REFERENCES	36
APPENDIX	42

1. INTRODUCTION

The popular assumption that speciation is manifested as physical change has recently come under scrutiny, since an increasing number of marine species have been demonstrated to share analogous ecological traits and similar morphological patterns (Bickford et al. 2007). This phenomenon appears common among elasmobranchs (class Chondrichthyes), whose deep genetic partitions suggest cryptic speciation events across several taxa, as documented within Rajiformes, family Rhinobatidae (Sandoval-Castillo et al. 2004) and Rajidae (Griffiths et al. 2010), Myliobatiformes, family Myliobatidae and Dasyatidae (Pavan-Kumar et al. 2013; Henderson et al. 2015), Carcharhiniformes, family Sphyrnidae (Quattro et al. 2006) and Carcharhinidae (Ovenden et al. 2011).

Here I examined and discussed the case of *Raja miraletus* (L.) species complex, whose connectivity, population structure and evolutionary history suggested its tripping into past cryptic speciation.

The Brown skate is a demersal cartilaginous fish of small-medium size (from average length 20-50cm to max length 60cm; McEachran et al. 1998) belonging to the family Rajidae and superorder Batoidea. The latter diversified into Torpediniformes, Pristiformes, Myliobatiformes and Rajiformes during the Jurassic period (Tinti, 2008), when the shark body plan, typical of ancestral Neoselachians (Shirai, 1996), independently evolved into a depressed, rounded pectoral disk supported to the snout tip by fin radials (Aschliman et al. 2012).

R. miraletus (etymology *Raja*: Latin, raja,-ae) is characterized by a wide distribution: it can be found along the Atlantic Coasts from Spain and Morocco to South Africa and the South-West Indian Ocean (IUCN, 2009; Fig.1), within the Mediterranean Basin at a depth range between 17m and 462m (Mytilineou et al. 2005) and mostly over soft bottoms. The species inhabits also the Black Sea (Stehmann and Bürkel, 1984; Compagno and Ebert, 2007; Froese and Pauly, 2015) and has also been reported along the Northern and Southern coastline of Portugal, although nowadays its presence seems to be more and more rarefied (Serra-Pereira et al. 2010).



Figure 1. Geographical distribution of *R. miraletus*.

R. miraletus is recognizable by its morphology and peculiar pigmentation: the body shape is rhomboid, starting with a slightly pointed and short snout and finishing with a long tail. The tail has small thorns, two small dorsal fins and a small caudal fin on its end. In Italy *R. miraletus* is commonly known as “Razza quattrocchi”, owing its name to a distinctive feature of this species: on the upper ochre-brownish surface scattered with dark spots (Stehmann and Bürkel, 1984; Compagno et al. 1989), two bright blue-purple eyespots encircled with one yellow line (*ocellus*) stand clearly out at the base of both pectoral fins (Fig.2). The ventral portion is white, non-pigmented and smooth.

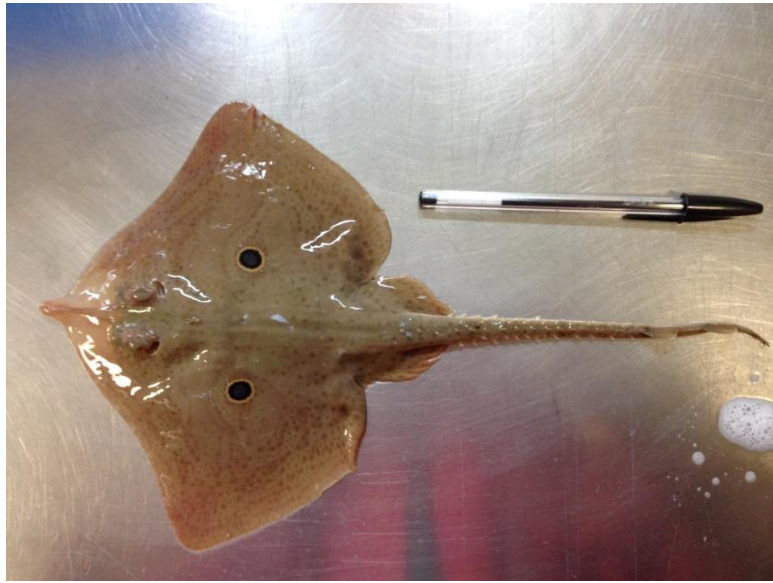


Figure 2. Immature individual of *R. miraletus* caught in the Sicilian Channel during the MEDITS survey of 2014.

The Brown skate has been included in the IUCN Red List of Threatened species in 2009 (Smale et al. 2009, classified as Least Concern) since, similarly to many other elasmobranchs, it is characterized by a slow reproduction rate and a low recovery after disturbance. Besides the sensitive ecological and biological traits (scarcely migratory and ovoviviparous), this species suffers from by-catch of bottom trawl fisheries, with significant differences depending on the gears and areas considered.

Historical data collected during GRUND and MEDITS scientific surveys between 1994 and 2011 in the Italian Waters have shown that the Brown skate has been characterized by fluctuant and generally negative abundance and biomass indices in Tuscany (FAO division 37.1.3; see Fig.3), while in Southern Adriatic (FAO division 37.2.1) sexually mature individuals have been rarely caught. *R. miraletus* has been collected with a 14-30% frequency along the Sardinian Coasts (FAO division 37.1.3) and with a slightly lower frequency (12-25%) in the FAO division 37.2.2, corresponding to the Sicilian Channel (data from ELASMOSTAT final report, ARPAT).

For this reasons the improvement and implementation of a species-specific stock assessment, management plans and catch monitoring are strongly recommended in order to guarantee its conservation and recovery.

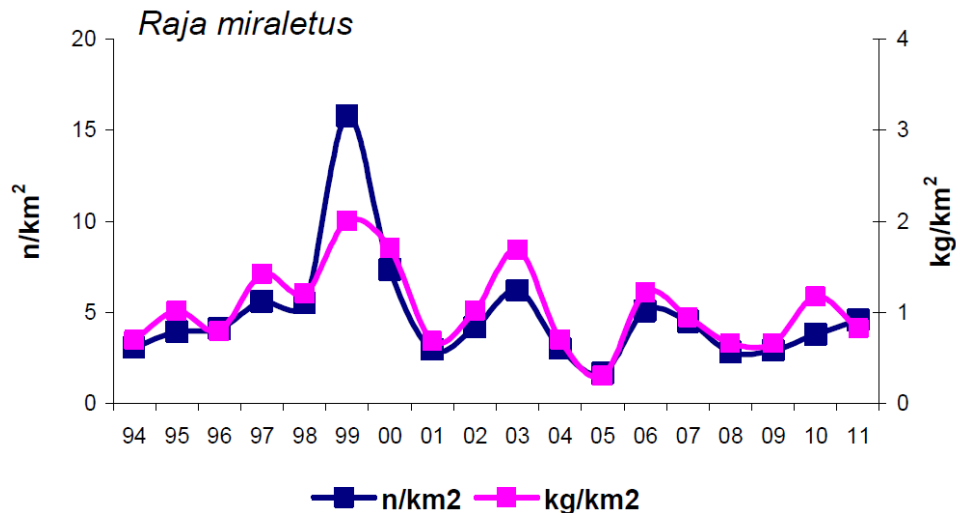


Figure 3. *Raja miraletus* indices of density (n/km²) and biomass (kg/km²) estimated in the Tuscany distribution area (MEDITS 1994-2011 series). Data from ELASMOSTAT final report, ARPAT.

Considering the wide distributional area of the Brown skate and both thermal gradients and currents crossings characterizing the Atlantic Coast of Africa in first place, we can distinguish three main biogeographical regions in the species range (Briggs, 1974). The North-Western region comprehends the area from the Strait of Gibraltar to Cape Blanco (21°N). Many oceanic currents from the Mediterranean Sea characterize this province (i.e. the inter-tropical Canary Current) and Cape Blanco is therefore the southern range limit for many endemic Mediterranean species. The upwelling zones of Cape Blanco and Cape Frio (18°S) bound the tropical, central region, under which the Benguela front is localized. Cape Frio receives the cold waters from the Benguela Current coming from the Antarctic. The third region ranges from Cape Frio to Cape Agulhas, where the Indian-warm Agulhas Current replaces the Benguela Current.

In second instance, the variety of hydrological and climatic condition found throughout the Mediterranean Sea (Bianchi and Morri, 2000) and the past and present connections with adjacent oceans and basins, e.g. with the Atlantic and Indian Oceans throughout the Gibraltar Strait and the Suez Channel respectively and with the Black Sea throughout the Bosphorus-Dardanelles sill (Boero, 2003; Abdulla et al. 2008; Coll et al. 2010), could have also influenced population structuring of this species within the basin. Particular attention should be paid to the oceanographic and hydrographic discontinuities characterizing the Mediterranean Sea. The southern limit of its continental shelf can be considered a continuous *couloir* connecting the westernmost part of the Basin to the centre-south (Algeria, Sardinia, Tuscany and Sicily). In particular, both Sicilian Channel and Ionian Sea represents a meeting point between Western and Eastern Basin and are known to be a sensitive transition district, due to a slow replacement of water. The Sicilian Channel is a morphologically complex area because of its particular geological development, oceanographic dynamics and for the physical, chemical, biological processes characterizing it (Betroux, 1980; Manzella et al. 1988; Robinson et al. 1999; Garcia Lafuente et al. 2002). Within the Channel, two banks can be distinguished: Adventura and Maltese Bank (Fig.4a). These two submerged panhandles connect North Africa to Sicily and are crossed by two currents, the “Modified Atlantic Water” (Warn-Varnas et al. 1999) and the “Levantine Intermediate Water” (henceforth MAW and LIW; Bryden et al. 1994; Tsimplis and Bryden, 2000). The

superficial circulation of the Mediterranean Sea is strongly influenced by the incoming MAW (through the Strait of Gibraltar). This current is relatively warm and slightly salty (15°C, 36.2‰). On the other hand, the density of the “Levantine Surface Water” (LSW), which increases during the winter and enhances deep mixing events, calls cold and salty water (13.5°C, 38.4‰) known as LIW (Bryden et al. 1994; Tsimplis and Bryden, 2000). In the westernmost part of the Sicilian Channel the MAW forks into the “Atlantic Ionian Stream” (AIS) which carries Atlantic warmer and less salty water towards the Ionian Sea and the “Atlantic Tunisian current” (ATC) that flows in direction of the Tunisian Coast (Robinson et al. 1999; Lermusiaux and Robinson, 2001; Beranger et al. 2005). In addition, the AIS coming from the West brings two cyclonic vortices: the first on Adventura Bank and the second around the Maltese platform, at South of Capo Passero, where the internal water temperature is much lower than the offshore waters (Dinieri, 2008; Fig.4b). This current path is responsible for an upwelling zone, affecting the surface temperature and modifying the thermocline’s structure (Lermusiaux, 1998; Robinson et al. 1999).

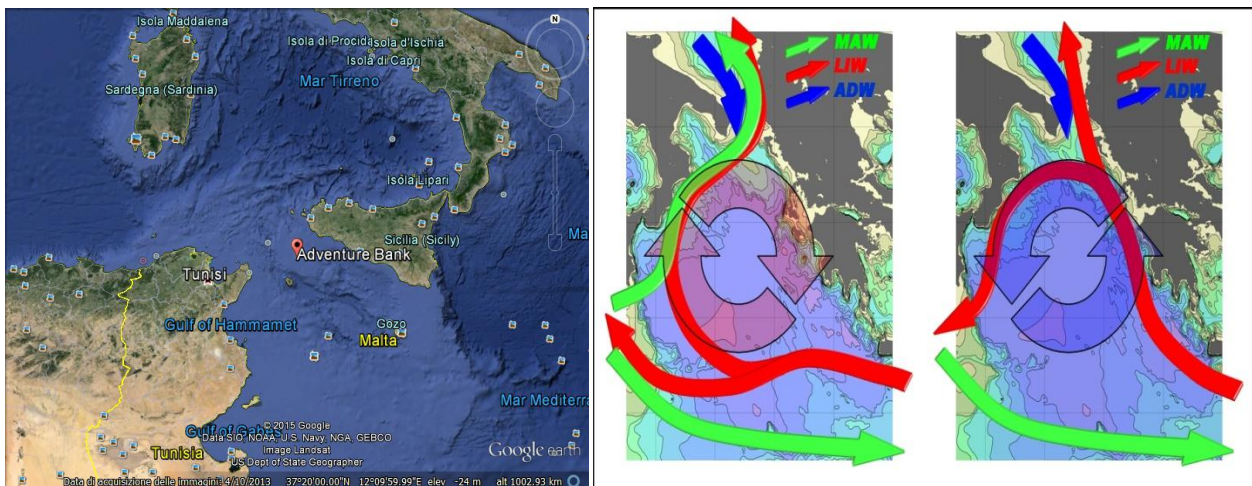


Figure 4a (left panel). Zoom on Sicilian Channel and localization of Adventura Bank and Maltese Bank.

Figure 4b (right panel). Superficial and deep inversions characterizing the Ionian Waters.

Since oceanographic and hydrographic discontinuities (i.e. upwelling zones) have been universally recognized as concomitant factors shaping population structure and regulating gene flow in the marine realm (Patarnello et al. 2007; Quinteiro et al. 2007; Galarza et al. 2009), this complex of transitional areas likely represents the most important migration barriers for small-sized fish and especially for the bottom dwelling elasmobranchs inhabiting the African and Mediterranean continental shelf and slope.

Twenty years after Wallace’s revision of the African skates’ taxonomy (Wallace, 1967), in which the South African *R. ocellifera* (Regan, 1906) population has been synonymised as *R. miraletus*, McEachran et al. (1989) started focusing their interest on the study of morphological characteristics of this species. In the mentioned case study, 124 specimens were collected along the Western and South African Coasts and within the Mediterranean Sea. After selecting 22 landmarks and comparing individual-based measurements, they could observe that the Gulf of Guinea-equatorial African samples partially overlapped with the Angolan sample, while the Mediterranean and South African could be considered morphologically distinct (Fig.5a

and Fig.5b), questioning Wallace's taxonomical incorporation of *R. ocellifera* into *R. miraletus* nominal species. As a matter of fact, the variation of meristic and morphometric characteristics of the Brown skate over this broad area supports the identification of three allopatrically or parapatrically distributed geographical populations: one inhabiting the Atlantic Coasts of South Africa, one belonging to Western Africa and one inhabiting the Mediterranean Sea (McEachran et al. 1989).

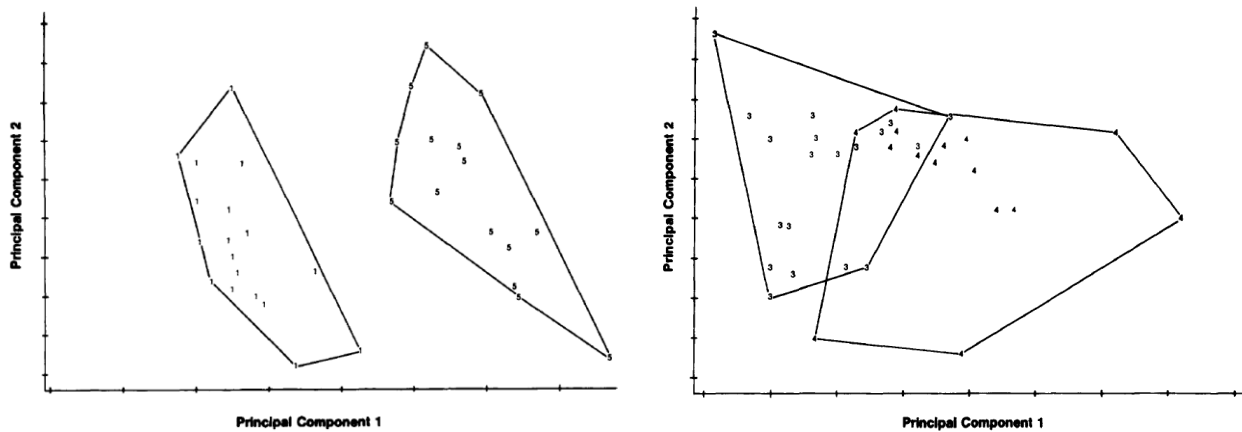


Figure 5a (left panel). Scatter of scores on the first two principal components of the Mediterranean and South African samples of *Raja miraletus*. 1=Mediterranean sample, 5=South African sample (analysis based on 22 log-transformed morphometric ratios; figure from McEachran et al. 1989).

Figure 5b (right panel). Scatter of scores on the first two principal components of the Gulf of Guinea-equatorial African and Angolan samples of *Raja miraletus*. 3=Gulf of Guinea-equatorial African sample, 4=Angolan sample (analysis based on 22 log-transformed morphometric ratios; figure from McEachran et al. 1989).

Skates and rays exhibit high levels of morphological and ecological stasis (Ebert and Compagno, 2007), which is paired with extraordinary species diversity. The complex mechanism of species evolution can be measured at different levels, morphology, genetic diversity and differentiation. *R. miraletus* represents another example of how strictly connected the environment, the behavioural habits and the evolutionary and ecologic drivers are.

The reported morphological variation of the Brown skate is coupled with the geographical clustering of highly divergent mitochondrial lineages (Cadinu, 2009; Cariani et al. 2010; Messinetti, 2013). At the same time high molecular divergence between populations of *R. miraletus* is also supported by nuclear loci (Cariani et al. 2012; Ferrari, 2012; Vinjau, 2012) that have detected strong genetic differences among geographical groups. For these reasons we hypothesized that the nominal *R. miraletus* likely followed cryptic speciation events, where the morphological similarity among taxa could be due to common descent (i.e. homologies), to convergent evolution (i.e. homoplasious character states), or both (Bernardo, 2011).

1.1. AIMS

On the basis of the mentioned observations I measured the genetic variation derived from both mitochondrial and nuclear markers (henceforth mtDNA and nuDNA) aiming to unravel the connectivity and the population structure of the target species *Raja miraletus*.

In particular I aim to investigate:

- 1) The species boundaries in *R. miraletus* complex, assessing the effectiveness of oceanographic barriers of Cape Frio and Cape Blanco;
- 2) The population boundaries in *R. miraletus* complex in Mediterranean Sea, verifying the occurrence of transitional areas or barriers to gene flow;
- 3) The role of ecological and environmental drivers in drawing the phylogeography of this species complex;
- 4) The demographical history of this species complex, assessing the origin time of its lineages/species.

2. MATERIALS AND METHODS

2.1. SAMPLING

In order to extend and integrate two previously analyzed and independent datasets from Ferrari (2012) and Vinjau (2012), a dedicated sampling activity was organized in the framework of the MEDITS survey in 2014. Fin clips from 19 *Raja miraletus* specimens were collected in December 2014 in the Adventura Bank area (Sicilian Channel). Fin clips were cut from each individual using sterile tweezers and clippers, transferred to a clean tube with 96% ethanol and stored at -20°C for subsequent DNA analyses. The final sample size for downstream analyses consisted of 338 individuals, collected during previous research project over a broad geographical area (South African, Senegalese, Angolan and Portuguese Coasts and the whole Mediterranean Sea; refer to Tab.1 and Fig.6 for collection details).

Sampling data								
FAO division	Area	N	N (SSR)	N (COI)	Years	Code	Source	Coordinates
Middle Agulhas 47.2.1	South Coast	8	8	5	2006	SAC/07	ST	Not available
Middle Agulhas 47.2.1	South Africa	0	0	5	2007	SAC/07	BOLD	33°68'S 26°86'E
Middle Agulhas 47.2.1	South Coast	32	31	30	2011	SAC/11	ST	20°19'S 36°57'E
Cunene 47.1.3	Angola	28	26	27	2006	ANC/06	ST	12°23'S 13°22'E
Cape Verde 34.3.1	Senegal	5	5	5	2007	SEC/07	LF	Not available
Portuguese Waters East IXa	Portugal	10	3	11	2005, 2006, 2007	POC/07	LF	38°87'N 9°68'W
Balearic 37.1.1	Algeria	8	5	8	2002, 2003	AGC/03	LF	Not available
Balearic 37.1.1	Algeria	9	8	8	2009, 2010	AGC/10	LF	Not available
Balearic 37.1.1	Balearic Islands	19	16	19	2006	BIS/06	ST	Not available
Sardinia 37.1.3	Northern Sardinia	11	8	11	2002, 2005	SDC/05	ST	Not available
Sardinia 37.1.3	Tuscany	26	21	22	2005, 2006	TUC/06	ST	Not available
Sardinia 37.1.3	Tuscany	16	13	6	2008, 2010	TUC/10	ST	43°00'N 9°44'E
Ionian 37.2.2	Sicily Channel Adventura Bank	22	22	22	2014	ADV/14	ST	37°12'N 13°20'E
Ionian 37.2.2	Sicily Channel Maltese Bank	16	8	17	2000, 2002	MAL/02	ST	Not available
Ionian 37.2.2	Ionian Sea	4	4	3	2004	JON/04	ST	36°40'N 15°08'E
Adriatic 37.2.1	Northern Adriatic Sea	30	8	30	2000, 2002, 2004	FNC/04	ST	43°44'N 14°50'E
Adriatic 37.2.1	Northern Adriatic Sea	33	20	25	2006, 2007	FNC/07	ST	43°41'N 14°57'E
Ionian 37.2.2	Southern Adriatic West	20	20	16	2001, 2004	PGC/04	ST	Not available
Ionian 37.2.2	Southern Adriatic East	22	20	14	2004	ABC/04	ST	Not available
Aegean 37.3.1	Aegean Greece	0	0	2	2014	GRE/14	BOLD	39°12'N 23°00'E
Levant 37.3.2	Israelian Coasts	8	7	14	2009	ILC/09	LF	Not available
Levant 37.3.2	Levantine Sea	11	7	11	2009	TKC/09	LF	Not available

Table 1. Geographical samples and codes of *Raja miraletus* individuals considered in this study and corresponding FAO division and geographical coordinate, when available. *N* number of individuals analysed per area. *N(SSRs)* number of individuals considered for nuclear markers analysis, *N(COI)* number of individuals considered for mitochondrial markers analysis, *ST* sample collected by scientific trawl, *LF* sample collected by fishery landings, *BOLD* sequence retrieved from BOLD online database (<http://www.boldsystems.org>).

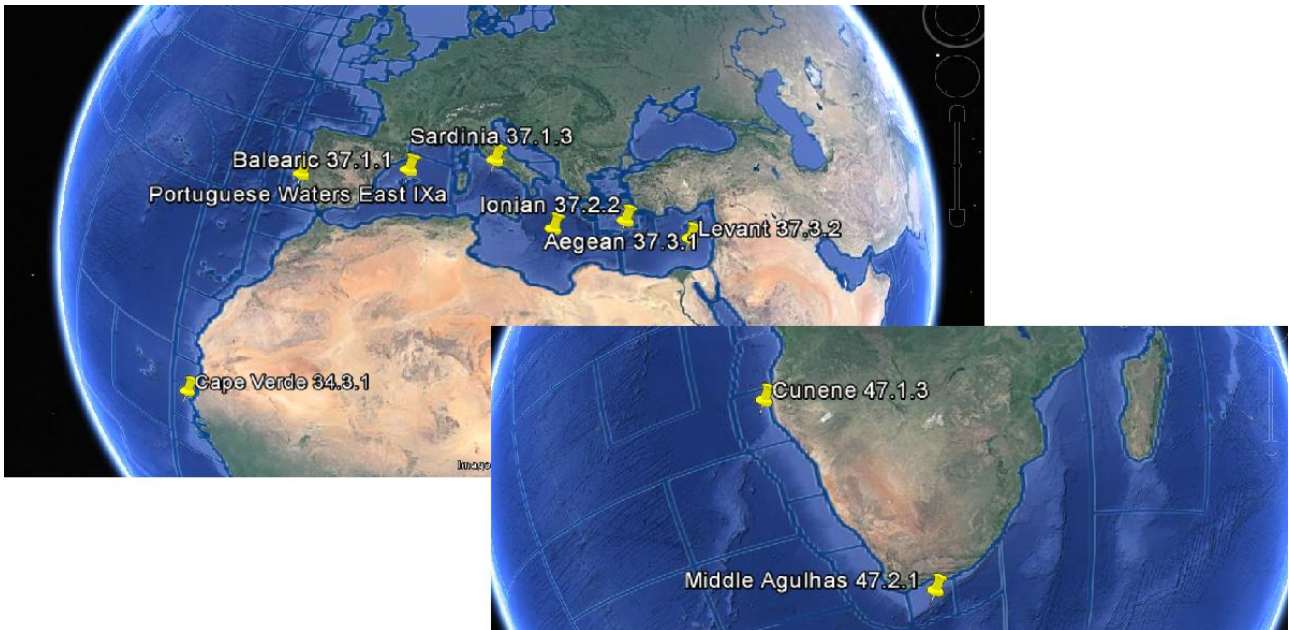


Figure 6. Sampling sites ranked per FAO division.

2.2. DNA EXTRACTION & PCR AMPLIFICATION

Total genomic DNA (gDNA) was extracted from about 20mg of each fin clip with the Invisorb® Spin Tissue Mini Kit (Stratec® molecular) according to manufacturer's protocol (for details visit http://www.stratec.com/en/molecular/Products_Molecular/Genomic_DNA/Invisorb_Spin_Tissue_Mini_Kit/Invisorb_Tissue_Mini.php).

2.2.1. Nuclear markers

Eight microsatellite loci (henceforth SSR loci) isolated and characterized in related species (El Nagar et al. 2010) and optimized in *R. miraletus* by Ferrari (2012) were used for the amplification of the 19 newly extracted gDNAs (Tab.2 in Appendix).

The PCR reactions were performed in a 10µL total volume containing 2-3µL of gDNA corresponding to ~20ng, 2µL of PCR Buffer (1X), 0.5µL of MgCl₂ (1.25mM), 0.5µL each primer (0.5µM), 0.8µL of dNTP mix (0.05mM each) and 1U Recombinant Taq DNA Polymerase (Promega).

DNA amplifications were run on a Biometra T-Gradient Thermocycler as follows: after an initial denaturation at 94°C for 3 min, amplification was performed with 30 cycles consisting of denaturation at 94°C for 30 sec, annealing at 53°C for 30 sec, extension at 72°C for 30 sec, followed by a final extension at 72°C for 10 min. Amplicons were checked on 2% agarose gel and successfully amplified fragments were stored at -20°C until shipping to Macrogen Europe (Amsterdam, the Netherlands). Individual genotyping was performed on ABI3100 Genetic Analyser (Applied Biosystems), using forward primers labelled and LIZ HD500 (Applied Biosystems) as internal size standard.

2.2.2. Mitochondrial marker

A fragment of the mitochondrial Cytochrome oxidase subunit I (COI) gene of about 650bp was amplified using the COI-3 primer cocktail (Ivanova et al. 2007; Tab.3 in Appendix) designed to increase the probability of primers' annealing to each of strand of DNA template.

PCR reactions were performed in 50µL total volume containing 10µl of buffer Promega (1X), 5µl MgCl (2.5mM), 0.5µl of dNTP mix (0.1mM each one), 1 µl of each primer (0.2mM), 0.25U Taq DNA Polymerase (Promega) and 4µl of pure gDNA. The cycle was planned with the following thermal profile: 94°C for 2 min, 35 cycles of 94°C for 30 sec, 52°C for 40 sec, 72°C for 1 min and a final extension step at 72°C for 10 min. The PCR products were visualized on agarose gel at 2% and successfully amplified fragments were stored at -20°C until shipping to Macrogen Europe (Amsterdam, the Netherlands). Individual Sanger sequencing was carried out on Applied Biosystems 3730xl DNA Analyzer.

2.3. DATA ANALYSIS

2.3.1. Nuclear markers dataset assessment

The 19 newly obtained chromatograms for each of the eight SSR loci were manually checked using GENEMAPPER v5.0 (Applied Biosystems). Furthermore, I have performed the careful revision, calibration and binning of two previous datasets (Ferrari, 2012; Vinjau, 2012), building a final dataset constituted by 260 individual genotypes. The allele calling for a total of 260 individuals has been realized through GENEMAPPER. The initial scoring of alleles provided size values as two decimal numbers. The software includes, besides the possibility to process quality values (PQVs), used to identify high, medium, and low quality data, also the binning of allelic values. In other words, it assigns an integer (*bin*) to the scored alleles according to their length in base pairs and rounds off the raw values. This software allows avoiding the introduction of errors in the allele-calling phase that could be undertaken through the manual correction of raw data and affect the estimates of genetic diversity and differentiation. Then, ML-NullFreq (Kalinowski et al. 2006) and FreeNA (Chapuis and Estoup, 2007) were used to test for the presence of stuttering, large allele drop out and null allele's artefacts.

2.3.2. Mitochondrial marker dataset assessment

A total of 38 forward and reverse strand electropherograms were manually edited and aligned by CLUSTAL W software (Thompson et al. 1994), incorporated into MEGA v.6.6 (Tamura et al. 2013). The correct amino acidic translation was assessed to exclude the presence of stop codons and sequencing errors (Moulton et al. 2010).

For each individual, consensus COI sequences were first compared with published sequences from both the Barcode of Life Data System (BOLD at <http://www.boldsystems.org>) and the NCBI (<http://www.ncbi.nlm.nih.gov/genbank/>) on-line databases through the BLAST algorithm (<http://blast.ncbi.nlm.nih.gov/Blast.cgi>) in order to rule out any error due to mishandling of samples on board

or during the laboratory activities. After this assessment, the newly obtained sequence were integrated in the existing dataset originated in previous research work (Cadinu, 2009; Bertucci Maresca, 2010; Vinjau, 2012). Available sequences for *R. miraletus* were also retrieved from both on-line databases selecting, when available, records from different geographical origins: South Africa and Aegean Sea. The retrieved sequences were integrated building a final dataset of 311 sequences.

2.3.3. Genetic diversity

The complete SSRs dataset was analysed using GENETIX v.4.05 (Belkhir et al. 2004) in order to estimate some descriptive statistics, as the observed heterozygosity (H_O), expected heterozygosity (H_E) Through Weir & Cockerham's F-statistics estimators, it was possible to apply the Jackknifing over loci to assess the single-locus effects. The deviation from the Hardy–Weinberg equilibrium (HW) was investigated using the exact tests from GENEPOP on the web v.4.2 (Rousset, 2008). The allelic richness (A_r) and the inbreeding coefficient were estimated using FSTAT v.2.9.3.2 (Goudet, 2002).

On the complete COI dataset, the number of polymorphic sites (S), the haplotype diversity (H_d), and the nucleotide diversity (π ; Nei, 1987) and their standard deviations were calculated using DNASP v.5.0 (Rozas et al. 2009). The best evolutionary substitution model was assessed using MEGA following the corrected Akaike Information Criterion (AICc; Akaike, 1977) and it was applied to all subsequent analyses. ARLEQUIN v.3.5.2.2. (Excoffier et al. 2010) was used to calculate the haplotype frequencies.

2.3.4. Population differentiation

F_{ST} and ϕ_{st} distance matrices were calculated using ARLEQUIN with 10,000 permutations, $P < 0.05$ and Tamura-Nei substitution model applied to the mtDNA dataset. The virtual spatial differentiation and genetic relationships among geographical population samples were assessed through Principal Coordinate Analysis (PCoA) and were conducted on Genotypic and Haploid Genetic Distance matrix. PCoA plots were generated using the program GenALEX v.6.5 (Peakall and Smouse, 2012). The genetic heterogeneity among the geographic samples was also assessed by the analysis of molecular variance (AMOVA, Excoffier et al. 1992). Different grouping of the geographic samples were tested, following both *a priori* subdivision according to sampling locations and FAO divisions as well as according to the groups revealed by the PCoA results. The adjustment of p -values has been realized through the sequential Bonferroni correction (Rice, 1989) implemented in the software SGoF+ (Carvajal-Rodriguez and de Uña-Alvarez, 2011).

In order to unravel the individual-based genetic clustering, I analysed two SRRs datasets, one considering the totality of the geographical samples and one focusing on NE Atlantic-Mediterranean samples, using the Bayesian algorithm implemented in STRUCTURE v2.3.4 (Falush et al. 2007). This analysis was carried out assuming an admixture ancestry model with the geographical origin of samples as prior information (LOCPRIOR models), associated with a correlated allele frequencies model. For each simulation of K (1-20), five independent replicates were run, setting a burn-in period of 200,000 iterations and 500,000 iterations for the MCMC. The assessment of the number of cluster K was inferred using Evanno's Δk and

Pritchard's average log probability methods (Pritchard et al. 2000, Evanno et al. 2005), both implemented in the STRUCTURE HARVESTER v.0.6.93 web application (Earl and Von Holdt, 2012).

To investigate haplotype relationships, the parsimony network was created using HAPLOVIEWER (<http://www.cibiv.at/~greg/haploviewer>) and the *dnapars* program of the PHYLIP package version 3.6 (Felsenstein, 2005).

The average genetic distances observed within and between the Atlantic African and the NE Atlantic-Mediterranean clades were calculated using MEGA and compared with inter-groups distances of homologous COI sequences (529bp) of different species of Rajidae (*Raja straeleni*, *R. microocellata*, *R. asterias*, *R. brachyura*, *R. clavata*, *R. montagui*, *R. polystigma*, *R. radula* and *R. undulata*) retrieved from the NCBI (<http://www.ncbi.nlm.nih.gov/genbank/>) on-line database. The best model used was the Tamura Nei model.

2.4. DEMOGRAPHIC HISTORY

The time at which the siblings African (ex *R. ocellifera*) and Mediterranean *R. miraletus* diverged was estimated using a Bayesian coalescent approach, as implemented in BEAST v1.8 (Drummond and Rambaut, 2012). In order to estimate the most recent common ancestor (TMRCA) we included the complete COI dataset and a sub-set of NE Atlantic-Mediterranean *R. miraletus*. A strict clock and a Yule tree prior were used. I set the normal prior distribution probabilities with mean 12 MYA for the whole COI dataset, 5.5 MYA for the NE Atlantic-Mediterranean clade and SD=1. This calibration was based on the time of rising of species diversity among the NE Atlantic and Mediterranean Sea, determined by Valsecchi et al. (2005) using mtDNA 16S sequence divergence scaled with fossil records was used by placing a normal distribution on the root height. For this analysis we applied the TN93 substitution model, as the most appropriated model inferred by MEGA software. To ensure convergence of the posterior distributions a Markov Chain Monte Carlo (MCMC) run of 30,000,000 generations sampled every 1,000 generations with the first 25% of the sampled points removed as burn-in were performed and combined subsequently in the module LOGCOMBINER (BEAST software package).

3. RESULTS

3.1. Nuclear and mitochondrial markers dataset assessment

The final SRRs dataset analysed for *R. miraletus* was constituted by 260 individuals divided in 20 geographical populations, including 19 specimens collected in the Adventura Bank, 171 Mediterranean specimens previously considered by Ferrari (2012) and 70 specimens considered by Vinjau (2012). I performed a meticulous revision, calibration and binning of the complete dataset over all eight SRRs loci.

Similarly, a final dataset of 311 COI sequences over 21 geographical populations was obtained analysing new 38 forward and reverse strand electropherograms, aligning the resulting 19 consensus sequences and integrating them with those considered in Vinjau (2012).

3.2. Genetic diversity

3.2.1. Nuclear markers polymorphism

On average, all eight SSR loci were polymorphic, with a number of alleles ranging from eight (Leri34, Leri40 and Leri50) to 15 (Leri27). The allele frequencies at the 20 geographic samples are shown in Tab.Ia (in Appendix). The comparison of genetic diversity estimates in temporal replicates TUC/06 and TUC/10 revealed that locus Leri34 shifted from polymorphic to monomorphic because of alleles' loss and the mean allelic richness showed a slight reduction (TUC/06=1.268; TUC/10=1.000, Tab.Ib).

In Tab.4, mean Allelic richness ($A_{r_{mean}}$) estimates showed similar low values for each geographical sample. The most variable sample was the SEC/07 despite the low number of individuals analysed, followed by ABC/04 and ANC/06. A low polymorphism was detected in POC/07 that exhibited five monomorphic loci (Leri26, Leri34, Leri63, Leri40 and Leri44). The A_r measured per each locus is available in Appendix, Tab.Ib.

SAMPLES																				
	SAC/07	SAC/11	ANC/06	SEC/07	POC/07	AGC/03	AGC/10	BIS/06	SDC/05	TUC/06	TUC/10	ADV/14	MAL/02	JON/04	FNC/04	FNC/07	PGC/04	ABC/04	ILC/09	TKC/09
	N=8	N=31	N=26	N=5	N=3	N=5	N=8	N=16	N=8	N=21	N=13	N=22	N=8	N=4	N=8	N=20	N=20	N=20	N=7	N=7
All loci																				
<i>A_{mean}</i>	3.5000	3.2500	6.1250	3.8750	1.6250	2.0000	2.5000	2.3750	2.3750	3.0000	2.6250	2.8750	2.6250	1.8750	2.3750	2.8750	3.5000	5.3750	3.0000	2.1250
<i>Ar_{mean}</i>	1.5955	1.3530	1.5279	1.7241	1.2416	1.2969	1.5065	1.3569	1.3193	1.3538	1.3094	1.3170	1.3305	1.3966	1.3750	1.4055	1.5014	1.5783	1.5313	1.3641
<i>H_{O mean}</i>	0.2656	0.2798	0.4044	0.6188	0.0417	0.2208	0.2359	0.2104	0.0729	0.1057	0.1406	0.2695	0.3125	0.2917	0.4063	0.2471	0.2453	0.2844	0.3571	0.1786
<i>H_{E mean}</i>	0.5519	0.3469	0.5175	0.6344	0.2014	0.2597	0.4679	0.3451	0.2977	0.3440	0.2968	0.3097	0.3084	0.3438	0.3516	0.3939	0.4871	0.5618	0.4814	0.3380
<i>FIS_{mean}</i>	0.5740	0.2100	0.2380	0.1940	0.8570	0.2810	0.5550	0.4190	0.7840	0.7070	0.5560	0.1530	0.0580	0.3000	-0.0900	0.3980	0.5180	0.5160	0.3490	0.5290
<i>HWE</i>	0.0000*	0.0000*	0.0000*	1.5895	0.0627	0.4225	0.0180*	0.0000*	0.0000*	0.0000*	0.0000*	0.0045*	0.1312	0.8090	0.0046*	0.0000*	0.0000*	0.0000*	0.0545	0.0089*

Table 4. Summary statistics of the SSR polymorphism per geographical sample and over all the loci considered. *A_{mean}* mean number of alleles, *Ar_{mean}* mean allelic richness, *H_{O mean}* mean observed heterozygosity, *H_{E mean}* mean expected heterozygosity, *FIS_{mean}* mean FIS value, *HWE* deviation from Hardy-Weinberg equilibrium. *P significant after sequential Bonferroni.

The comparisons between the expected (H_E) and observed (H_O) heterozygosity showed that H_E was higher than H_O in most samples and a significant deviation from HW equilibrium was detected in almost all samples, even after Bonferroni correction (Tab.4). The deviation from HW equilibrium was ascribed by low polymorphism and deficit of heterozygosity as confirmed by medium-high FIS values.

MI-Nullfreq and FreeNA results detected the presence of null alleles at loci Leri40, Leri50 and Leri44. Nevertheless we did not exclude any of them, since Jackknife analysis didn't reveal outliers over the confidence interval (Fig.7).

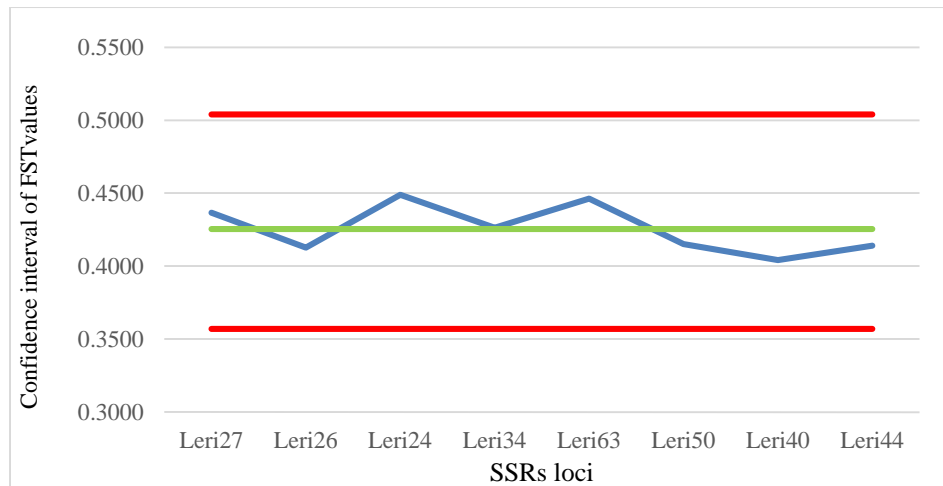


Figure 7. Jackknifing over loci.

3.2.2. Mitochondrial marker polymorphism

The COI polymorphism among 21 geographical samples and 311 sequences showed low nucleotide diversity (π), and very high haplotype diversity (H_d). The majority of samples showed medium-high values of H_d (Tab.5). ANC/06 showed the highest polymorphism, k estimate (13.453) and N_h (10), followed by ALG/10, ADV/14 and MAL/02. These geographical populations showed high values of H_d and π in relation to other samples. In general, the samples belonging to Eastern Mediterranean (JON/04, FNC/04, FNC/07, PGC/04, ABC/04, GRE/14, ILC/09, TKC/09) showed lower N_h , H_d and π values than those from NE Atlantic and Western Mediterranean (POC/07, AGC/03, AGC/10, BIS/06, SDC/05, TUC/06 and TUC/10). From the geographical distribution of the 38 haplotypes African and NE Atlantic-Mediterranean samples did not share any haplotype (Appendix, Tab.II). Hap_24 appeared common to 11 Mediterranean samples. The majority of haplotypes (26) was detected in turn in only one population.

COI							
Species	Location	N	Nh	S	Hd \pm SD	π \pm SD	k
<i>Raja miraletus</i>							
	SAC/06/07	10	4	4	0.6440 \pm 0.1520	0.0020 \pm 0.0006	0.9556
	SAC/11	30	8	6	0.7330 \pm 0.0660	0.0020 \pm 0.0003	1.0874
	ANC/06	27	10	40	0.8580 \pm 0.0410	0.0254 \pm 0.0040	13.4530
	SEC/07	5	3	1	0.7000 \pm 0.2180	0.0013 \pm 0.0004	0.7000
	POC/07	11	1	0	0.0000	0.0000	0.0000
	AGC/03	8	1	0	0.0000	0.0000	0.0000
	AGC/10	8	4	4	0.7500 \pm 0.1390	0.0025 \pm 0.0004	1.3214
	BIS/06	19	1	0	0.0000	0.0000	0.0000
	SDC/05	11	1	0	0.0000	0.0000	0.0000
	TUC/06	22	2	1	0.0910 \pm 0.0810	0.0002 \pm 0.0001	0.0909
	TUC/10	6	1	0	0.0000	0.0000	0.0000
	ADV/14	22	3	3	0.6540 \pm 0.0610	0.0028 \pm 0.0004	1.4632
	MAL/02	17	6	6	0.8010 \pm 0.0650	0.0033 \pm 0.0004	1.7353
	JON/04	3	1	0	0.0000	0.0000	0.0000
	FNC/04	30	5	4	0.5840 \pm 0.0660	0.0013 \pm 0.0002	0.6805
	FNC/07	25	2	1	0.4200 \pm 0.0820	0.0008 \pm 0.0001	0.4200
	PGC/04	16	3	2	0.2420 \pm 0.1350	0.0007 \pm 0.0004	0.3583
	ABC/04	14	2	1	0.3630 \pm 0.130	0.0007 \pm 0.0002	0.3636
	GRE/14	2	1	0	0.0000	0.0000	0.0000
	ILC/09	14	2	1	0.5270 \pm 0.0640	0.0010 \pm 0.0001	0.5275
	TKC/09	11	1	0	0.0000	0.0000	0.0000
Tot. All sequences		311	38	76	0.8560 \pm 0.0130	0.0270 \pm 0.0018	14.3281
Tot. Mediterranean		239	16	16	0.7650 \pm 0.0170	0.0025 \pm 0.0001	1.3444

Table 5. mtDNA polymorphism and its parameters. *Nh* number of haplotypes, *Hd* haplotype diversity, π nucleotide diversity, *k* average number of nucleotide differences, *S* number of polymorphic sites and *SD* standard deviation.

3.3. Population differentiation

It is important to note that small sample sizes, as those we deal with in several geographical samples, decrease the power of the analyses and consequently reduce the ability to detect significant population structure (Chevolot et al. 2006b); therefore, appropriate caution should be used in interpreting the results obtained. However, similar experimental designs and analytical approaches proved geographical population structure and genetic differentiation at multiple taxonomic levels in other skates (Chevolot et al. 2006a; Plank et al. 2010; Pasolini et al. 2011).

The analysis of genetic differentiation among 20 samples based on SSRs data showed significant pair-wise F_{ST} values ($P < 0.05$), even after Bonferroni correction (Tab.6).

	SAC/06	SAC/11	ANC/06	SEC/07	POC/07	AGC/03	AGC/10	BIS/06	SDC/05	TUC/06	TUC/10	ADV/14	MAL/02	JON/04	FNC/04	FNC/07	PGC/04	ABC/04	ILC/09	TKC/09
SAC/06	*	0.1524	0.2038	0.0178*	0.0048*	0.0006*	0.0005*	0.0000*	0.0035*	0.0000*	0.0000*	0.0000*	0.0002*	0.0082*	0.0160*	0.0000*	0.0000*	0.0000*	0.0000*	0.0005*
SAC/11	0.0802	*	0.0000*	0.0117*	0.0003*	0.0000*	0.0000*	0.0000*	0.0000*	0.0000*	0.0000*	0.0000*	0.0000*	0.00099*	0.0067*	0.0000*	0.0000*	0.0000*	0.0001*	0.0000*
ANC/06	0.0457	0.1965*	*	0.0019*	0.0001*	0.0000*	0.0000*	0.0000*	0.0000*	0.0000*	0.0000*	0.0000*	0.0000*	0.0000*	0.0001*	0.0000*	0.0000*	0.0000*	0.0000*	0.0000*
SEC/07	0.1926*	0.2246*	0.2559*	*	0.0198*	0.0062*	0.0146*	0.0004*	0.0137*	0.0001*	0.0003*	0.0000	0.0004*	0.0071*	0.1738	0.0015*	0.0032*	0.0660	0.0687	0.0445*
POC/07	0.5409*	0.4944*	0.5134*	0.4339*	*	0.9999	0.9999	0.5704	0.7785	0.6497	0.9999	0.9999	0.9999	0.0290*	0.1260	0.0005*	0.0021*	0.0012*	0.0077*	0.0090*
AGC/03	0.5952*	0.5183*	0.5392*	0.5139*	0.0000	*	0.9999	0.5322	0.4875	0.4220	0.9999	0.9999	0.9999	0.0085*	0.0207*	0.0000*	0.0001*	0.0001*	0.0042*	0.0011*
AGC/10	0.5190*	0.4684*	0.4903*	0.3903*	-0.0260	0.0252	*	0.9999	0.9999	0.8716	0.7511	0.2631	0.9999	0.0052*	0.0299*	0.0000*	0.0000*	0.0000*	0.0012*	0.0003*
BIS/06	0.5697*	0.5012*	0.5249*	0.4554*	-0.0190	0.0231	-0.0492	*	0.3129	0.7832	0.4702	0.0822	0.2547	0.0001*	0.0004*	0.0000*	0.0000*	0.0000*	0.0000*	0.0000*
SDC/05	0.4496*	0.4115*	0.3988*	0.3725*	0.0857	0.1444	0.0095	0.0244	*	0.2488	0.2827	0.1175	0.4694	0.0076*	0.0859	0.0000*	0.0000*	0.0002*	0.00198*	0.0007*
TUC/06	0.6103*	0.5199*	0.5455*	0.5186*	-0.0173	0.0226	-0.0408	-0.0243	0.0309	*	0.7082	0.0767	0.2894	0.0002*	0.0002*	0.0000*	0.0000*	0.0000*	0.0000*	0.0000*
TUC/10	0.6074*	0.5212*	0.5444*	0.5289*	-0.0721	-0.0301	-0.0198	-0.0056	0.0447	-0.0212	*	0.5359	0.4976	0.0014*	0.0012*	0.0000*	0.0000*	0.0000*	0.0000*	0.0000*
ADV/14	0.7755*	0.6080*	0.6399*	0.7507*	0.0000	0.0000	0.1089	0.0725	0.3112	0.0634	-0.0138	*	0.9999	0.0002*	0.0001*	0.0000*	0.0000*	0.0000*	0.0000*	0.0000*
MAL/02	0.6524*	0.5438*	0.5675*	0.5937*	0.0000	0.0000	0.0667	0.0529	0.2000	0.0495	-0.0034	0.0000	*	0.0020*	0.0069*	0.0000*	0.0000*	0.0000*	0.0004*	0.0002*
JON/04	0.3553*	0.3770*	0.3895*	0.3538*	0.6778*	0.7428*	0.6072*	0.6380*	0.5826*	0.6756*	0.6864*	0.8973*	0.8012*	*	0.3910	0.0001*	0.0001*	0.0000*	0.0118*	0.0149*
FNC/04	0.1644*	0.1945*	0.2326*	0.1177	0.2829	0.3462*	0.2831*	0.3448*	0.2130	0.3695*	0.3646*	0.5622*	0.4121*	0.0761	*	0.0000*	0.0002*	0.0014*	0.0294*	0.0084*
FNC/07	0.6137*	0.5327*	0.5295*	0.4598*	0.8303*	0.8432*	0.7828*	0.7801*	0.7652*	0.7979*	0.8141*	0.8979*	0.8587*	0.7527*	0.5093*	*	0.7516	0.0201*	0.1930	0.4823
PGC/04	0.5847*	0.5166*	0.5117*	0.4148*	0.7896*	0.8053*	0.7448*	0.7473*	0.7232*	0.7669*	0.7807*	0.8714*	0.8239*	0.7187*	0.4726*	-0.0162	*	0.0411*	0.3014	0.4781
ABC/04	0.3241*	0.3525*	0.3168*	0.1122	0.5402*	0.5696*	0.5143*	0.5510*	0.4691*	0.5788*	0.5779*	0.6865*	0.6025*	0.4690*	0.2445*	0.0817*	0.0662*	*	0.4846	0.1973
ILC/09	0.3766*	0.3840*	0.3709*	0.1699	0.6063*	0.6601*	0.5722*	0.6106*	0.5374*	0.6503*	0.6541*	0.8273*	0.7154*	0.4910*	0.2157*	0.0625	0.0193	-0.0053	*	0.5846
TKC/09	0.4886*	0.4545*	0.4449*	0.3265*	0.8178*	0.8472*	0.7523*	0.7613*	0.7370*	0.7917*	0.8064*	0.9312*	0.8765*	0.6317*	0.3579*	0.0201	0.0286	0.0495	0.0250	*

Table 6. Pair-wise FST values (below the diagonal) and associated significance (above the diagonal). *P significant after sequential Bonferroni.

Medium-high and significant pair-wise fixation index ($P < 0.05$) testified a clear differentiation between two main macro-areas: the Atlantic African Coasts and NE Atlantic-Mediterranean Sea.

At the same time, within the NE Atlantic-Mediterranean samples, high and significant values were found. As a matter of fact, the Western Mediterranean (POC/07, AGC/03, AGC/10, BIS/06, SDC/05, TUC/06, TUC/10, ADV/14 and MAL/02) is significantly different from Eastern Mediterranean (FNC/07, PGC/04, ABC/04, ILC/09 and TKC/09).

Differently, the comparison within FNC/07, PGC/04, ABC/04, ILC/09 and TKC/09 was not significant.

The comparison of population differentiation estimates in temporal replicates AGC/03, AGC/10 and TUC/06, TUC/10 revealed low and not-significant FST values.

Furthermore, also the genetic differentiation among 21 samples based on COI data showed significant pair-wise Φ_{st} values, even after Bonferroni correction ($P < 0.05$; Tab.7). Φ_{st} values were in most cases more informative than those showed by the FST pair-wise matrix in detecting more genetic differentiations within the Western Mediterranean and the Eastern Basins. As a matter of fact, differently from FST values, Φ_{st} highlighted high and significant values within FNC/07, PGC/04, ABC/04, ILC/09 and TKC/09.

Coherently, the deeper differentiation was observed between Atlantic Africa and NE Atlantic-Mediterranean samples, but also between Western and Eastern Mediterranean.

	SAC/06/07	SAC/11	ANC/06	SEC/07	POC/07	AGC/03	AGC/10	BIS/06	SDC/05	TUC/06	TUC/10	ADV/14	MAL/02	JON/04	FNC/04	FNC/07	PGC/04	ABC/04	GRE/14	ILC/09	TKC/09
SAC/06/07	*	0.6436	0.0002*	0.0003*	0.0000*	0.0001*	0.0001*	0.0000*	0.0000*	0.0000*	0.0001*	0.0000*	0.0000*	0.0038*	0.0000*	0.0000*	0.0000*	0.0000*	0.0178*	0.0000*	0.0000*
SAC/11	-0.0252	*	0.0000*	0.0000*	0.0000*	0.0000*	0.0000*	0.0000*	0.0000*	0.0000*	0.0000*	0.0000*	0.0000*	0.0000*	0.0000*	0.0000*	0.0000*	0.0000*	0.0029*	0.0000*	0.0000*
ANC/06	0.3101*	0.4147*	*	0.0001*	0.0000*	0.0000*	0.0000*	0.0000*	0.0000*	0.0000*	0.0000*	0.0000*	0.0000*	0.0002*	0.0000*	0.0000*	0.0000*	0.0000*	0.0027*	0.0000*	0.0000*
SEC/07	0.9441*	0.9346*	0.4988*	*	0.0003*	0.0006*	0.0005*	0.0001*	0.0002*	0.0000*	0.0022*	0.0000*	0.0000*	0.0177*	0.0000*	0.0000*	0.0000*	0.0000*	0.0476*	0.0001*	0.0002*
POC/07	0.9878*	0.9784*	0.7352*	0.9951*	*	0.9999	0.0155*	0.0000*	0.0000*	0.0000*	0.0000*	0.0002*	0.0001*	0.0028*	0.0000*	0.0000*	0.0000*	0.0000*	0.0114*	0.0000*	0.0000*
AGC/03	0.9856*	0.9767*	0.7161*	0.9938*	0.0000	*	0.0733	0.0000*	0.0000*	0.0000*	0.0003*	0.0022*	0.0004*	0.0069*	0.0000*	0.0000*	0.0000*	0.0000*	0.0199*	0.0000*	0.0000*
AGC/10	0.9707*	0.9702*	0.7127*	0.9740*	0.3041*	0.2446	*	0.0001*	0.0010*	0.0001*	0.0864	0.0749	0.0426*	0.0224*	0.0003*	0.0001*	0.0000*	0.0000*	0.0646	0.0000*	0.0000*
BIS/06	0.9917*	0.9826*	0.7808*	0.9970*	1.0000*	1.0000*	0.4161*	*	0.9999	0.9999	0.9999	0.0000*	0.0000*	0.0008*	0.0000*	0.0000*	0.0000*	0.0000*	0.0043*	0.0000*	0.0000*
SDC/05	0.9882*	0.9791*	0.7427*	0.9953*	1.0000*	1.0000*	0.3041*	0.0000	*	0.9999	0.9999	0.0021*	0.0031*	0.0011*	0.0004*	0.0000*	0.0000*	0.0004*	0.0112*	0.0000*	0.0000*
TUC/06	0.9908*	0.9826*	0.7907*	0.9955*	0.9421*	0.9361*	0.3993*	-0.0069	-0.0359	*	0.9999	0.0000*	0.0000*	0.0005*	0.0000*	0.0000*	0.0000*	0.0000*	0.0040*	0.0000*	0.0000*
TUC/10	0.9840*	0.9760*	0.7092*	0.9926*	1.0000*	1.0000*	0.1928	0.0000	0.0000	-0.0845	*	0.0356*	0.0393*	0.0136*	0.0047*	0.0025*	0.0005*	0.0020*	0.0348*	0.0000*	0.0001*
ADV/14	0.9661*	0.9677*	0.7757*	0.9686*	0.4922*	0.4601*	0.1375	0.4048*	0.3384*	0.4107*	0.2754*	*	0.5547	0.2332	0.0004*	0.0004*	0.0003*	0.0039*	0.4062	0.0000*	0.0000*
MAL/02	0.9628*	0.9662*	0.7583*	0.9644*	0.5335*	0.4965*	0.1653*	0.3753*	0.2993*	0.3824*	0.2264*	-0.0231	*	0.2191	0.0018*	0.0017*	0.0013*	0.0071*	0.4545	0.0000*	0.0000*
JON/04	0.9803*	0.9745*	0.6872*	0.9893*	1.0000*	1.0000*	0.6034*	1.0000*	1.0000*	0.9601*	1.0000*	0.1940	0.1316	*	0.0004*	0.0000*	0.0011*	0.0030*	0.1051	0.0016*	0.0036*
FNC/04	0.9809*	0.9775*	0.8115*	0.9842*	0.7310*	0.7133*	0.3733*	0.4793*	0.4244*	0.4737*	0.3738*	0.2321*	0.1728*	0.6165*	*	0.5742	0.1160	0.4872	0.6335	0.0000*	0.0000*
FNC/07	0.9855*	0.9800*	0.8013*	0.9893*	0.8350*	0.8212*	0.4834*	0.6788*	0.6273*	0.6565*	0.5812*	0.2684*	0.2050*	0.7222*	-0.0177	*	0.1597	0.7201	0.5759	0.0000*	0.0000*
PGC/04	0.9851*	0.9787*	0.7700*	0.9900*	0.8906*	0.8771*	0.5410*	0.8231*	0.7774*	0.7896*	0.7327*	0.2914*	0.2259*	0.7515*	0.0627	0.0187	*	0.6474	0.9999	0.0000*	0.0000*
ABC/04	0.9846*	0.9781*	0.7606*	0.9898*	0.8866*	0.8713*	0.4815*	0.7999*	0.7456*	0.7574*	0.6912*	0.2478*	0.1805*	0.7579*	-0.0069	-0.0470	-0.0353	*	0.9999	0.0000*	0.0000*
GRE/14	0.9783*	0.9736*	0.6699*	0.9872*	1.0000*	1.0000*	0.3715	1.0000*	1.0000*	0.9187*	1.0000*	0.1200	0.0107	1.0000	-0.0608	-0.0817	-0.2871	-0.1756	*	0.0078*	0.0128
ILC/09	0.9834*	0.9785*	0.7746*	0.9876*	0.9334*	0.9240*	0.7973*	0.9350*	0.9141*	0.9252*	0.8922*	0.7099*	0.6849*	0.8717*	0.7841*	0.8306*	0.8330*	0.8321*	0.8069*	*	0.0000*
TKC/09	0.9888*	0.9802*	0.7567*	0.9955*	1.0000*	1.0000*	0.7853*	1.0000*	1.0000*	0.9702*	1.0000*	0.6030*	0.5665*	1.0000*	0.6866*	0.7815*	0.8234*	0.8342*	1.0000	0.9139*	*

Table 7. Pair-wise Φ_{st} values (below the diagonal) and associated significance (above the diagonal). *P significant after sequential Bonferroni.

The average genetic distance within groups of individuals belonging to the NE Atlantic-Mediterranean clade was very low (0.0025), indicating a certain degree of homogeneity. The same could not be observed within the Atlantic African clade (0.0187).

The inter-specific distances between the other skates species (Tab.8) have showed ranging values from Minimum 0.015 for the recently diverged species *Raja clavata*-*R. straeleni* and *R. montagui*-*R. polystigma* to Maximum 0.088 for *R. asterias*-*R. microocellata*. A high value (0.073) was exhibited by the relationship with *R. undulata* the species more phylogenetically distant between all (Messinetti, 2013).

Raja_straeleni									
Raja_microocellata	0.060								
Raja_asterias	0.060	0.088							
Raja_brachyura	0.060	0.045	0.088						
Raja_clavata	0.015	0.060	0.060	0.052					
Raja_montagui	0.058	0.062	0.082	0.058	0.050				
Raja_polystigma	0.056	0.064	0.080	0.051	0.052	0.021			
Raja_radula	0.029	0.067	0.050	0.071	0.029	0.064	0.062		
Raja_undulata	0.073	0.080	0.077	0.071	0.073	0.077	0.071	0.075	
	Raja_straeleni	Raja_microocellata	Raja_asterias	Raja_brachyura	Raja_clavata	Raja_montagui	Raja_polystigma	Raja_radula	Raja_undulata

Table 8. Inter-specific distances among different skate species.

Two PCoA (Principal Coordinate Analysis) based on the Genetic Distance matrix, computed on the SSRs dataset, were performed to assess the virtual spatial differentiation among geographical populations (Fig.8 and Fig.9).

PCo1 and PCo2 explained most of the variation (Fig.8: 71.87%; Fig.9: 66.77%). The PCo1 reported in Fig.8 showed a pattern of differentiation where the African samples (SAC/06, SAC/11, ANC/06 and SEC/07) are the most divergent from NE Atlantic and Western Mediterranean ones (POC/07, AGC/03, AGC/10, BIS/06, SDC/05, TUC/06 TUC/10, ADV/14 and MAL/02), while the Eastern Mediterranean (JON/04, FNC/04, FNC/07, PGC/04, ABC/04, ILC/09, TKC/09) are differentiated from the others according to PCo2.

Zooming inside the Mediterranean Basin (Fig.9) the PCo1 revealed a strong differentiation between NE Atlantic-Western and Eastern Mediterranean samples, with the exception of FNC/07 and JON/04, which are located in the transition between the two main groups.

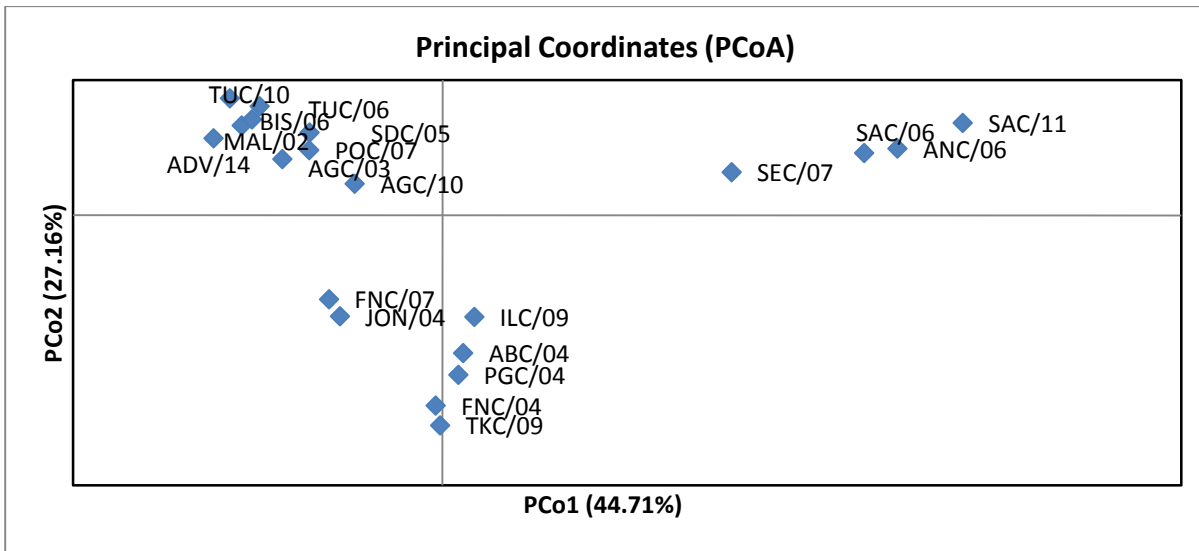


Figure 8. Plot describing the PCoA carried out on Genotypic Genetic Distance matrix over all geographical samples.

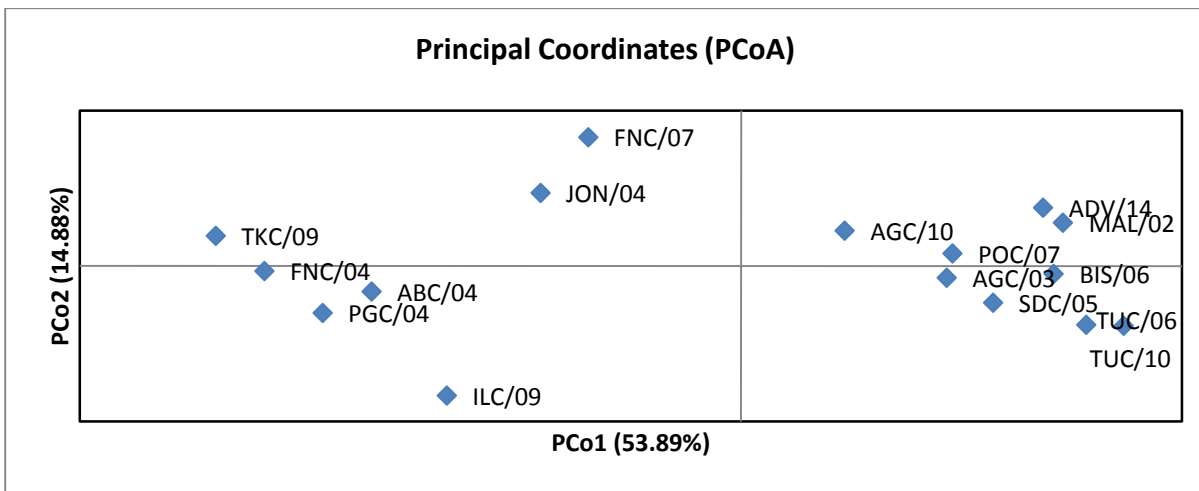


Figure 9. Plot describing the PCoA carried out on the Genotypic Genetic Distance matrix of NE Atlantic and Mediterranean

At the same way, PCoA (Principal Coordinate Analysis) based on the Haploid Genetic Distance, computed on the COI dataset, were performed (Fig.10 and Fig.11). Fig.10 showed a pattern of differentiation of two main groups: Atlantic Africa versus NE Atlantic-Mediterranean Sea, The PCo1 explained most of the variation (82.61%) and a total differentiation of the Senegalese sample (SEC/07).

The best performing PCoA was obtained comparing only the NE Atlantic-Mediterranean populations (Fig.11). The scatter plot showed three subgroups distributed along the PCo1, which explained 45.4% of variance. The differentiation between NE Atlantic-Western Mediterranean and Eastern Mediterranean was clear. According to PCo2, ILC/09 was the most differentiated sample.

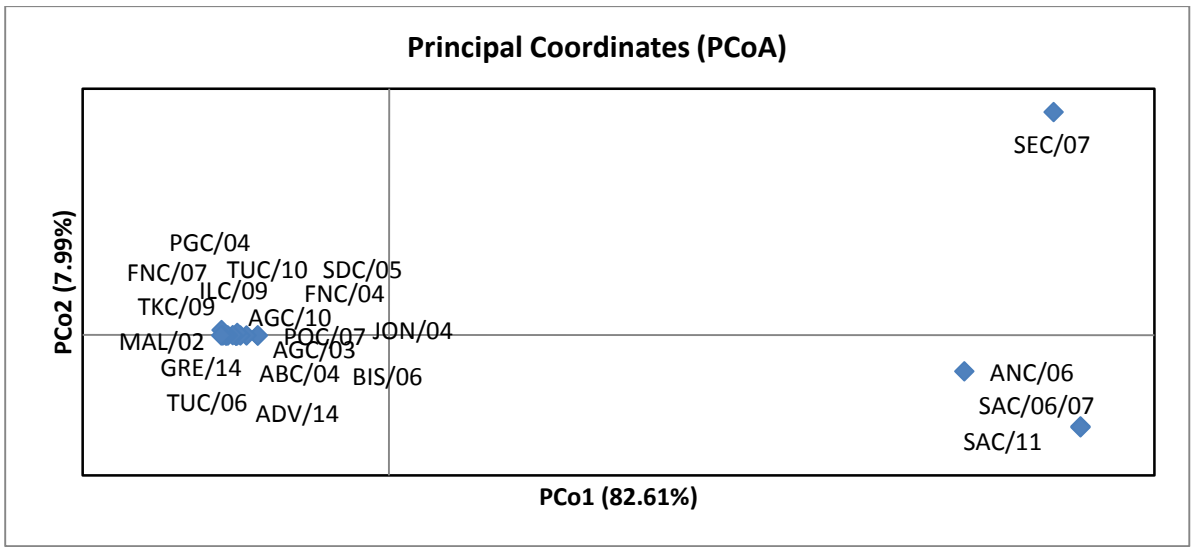


Figure 10. Plot describing the PCoA carried out on the Haploid Genetic Distance over all geographical samples.

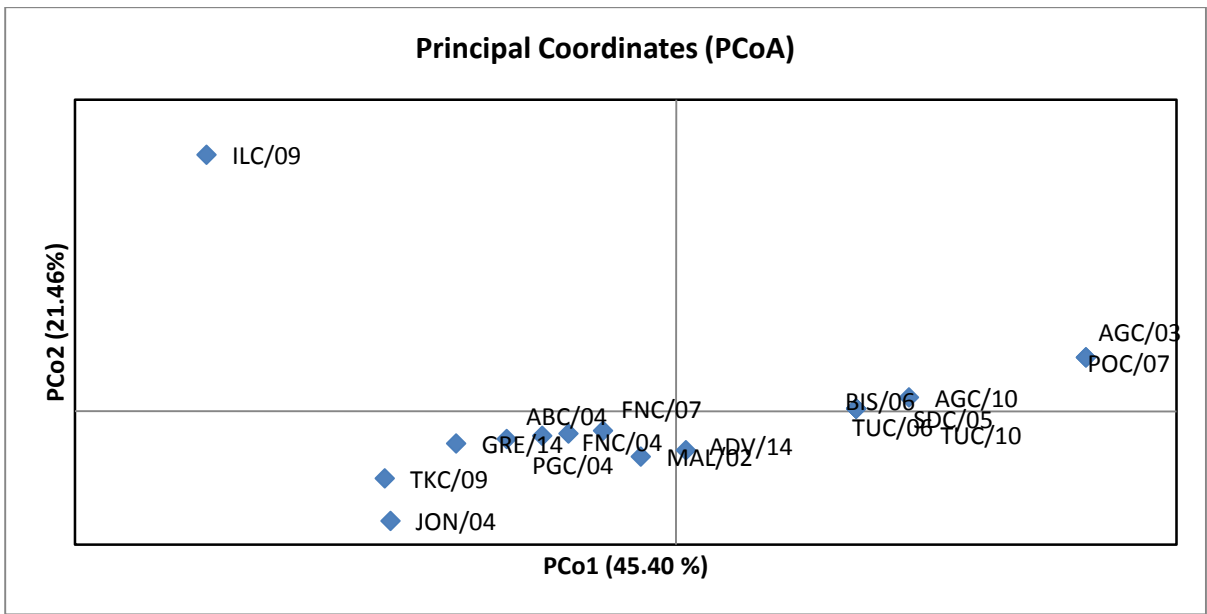


Figure 11. Plot describing the PCoA carried out on the Haploid Genetic Distance of NE Atlantic and Mediterranean samples.

The AMOVA analysis was performed on both SRRs and COI markers, testing three different sample groupings, set on the basis of geographical location of samples (FAO divisions) and on the PCoA results (Tab.9).

AMOVA1 was carried out over all samples, divided in two main groups defined on the geographic distance as: Atlantic Africa versus NE Atlantic-Mediterranean Sea (FAO divisions: Middle Agulhas, Cunene, Cape Verde versus Portuguese Waters East, Balearic, Sardinian, Ionian, Adriatic, Aegean, Levant).

AMOVA1 calculated on COI marker showed the highest and statistically significant percentage of molecular variation among groups (90.22%; FCT=0.90, P=0.0002).

AMOVA2 calculated on COI marker and two groups determined in view of the PCoA results carried out on the Genotypic Genetic Distance matrix (Portuguese Waters East, Balearic, Sardinian, Adventura and Maltese Bank versus Adriatic, Ionian, Aegean, Levant) showed 32.03% of variation among groups (FSC= 0.3203, P=0.0000; Fig.9). The same comparison calculated on SRRs markers showed a higher variation (more than 60%) and statistically significant value (FCT=0.6065, P=0.0000) among groups.

AMOVA3 focused on the Atlantic African samples and compared three groups: Middle Agulhas versus Cunene versus Cape Verde. Low/no variation was observed at any of the AMOVA levels, probably because of the small sample size (N) characterizing SEC/07.

AMOVA-Groupings	SSRs				AMOVA-Groupings	COI			
AMOVA1-All samples, two groups: Atlantinc Africa vs NE Atlantic-Mediterranean Sea	(Middle Aghulas, Cunene, Cape Verde) vs (Portuguese Waters East, Balearic, Sardinian, Jonian, Adriatic, Levant)				AMOVA1-All samples, two groups: Atlantinc Africa vs NE Atlantic-Mediterranean Sea	(Middle Aghulas, Cunene, Cape Verde) vs (Portuguese Waters East, Balearic, Sardinian, Jonian, Adriatic, Aegean, Levant)			
	Total variation (%)	<i>F</i> statistics		P		Total variation (%)	ϕ statistics		P
Among groups	22.2600	FCT	0.2226	0.0169+-0.0014	Among groups	90.2200	FCT	0.9022	0.0002+-0.0001
Among population within groups	36.3200	FSC	0.4672	0.0000+-0.0000	Among population within groups	4.7900	FSC	0.4903	0.0000+-0.0000
Within population	41.4200	FST	0.5858	0.0000+-0.0000	Within population	4.9800	FST	0.9502	0.0000+-0.0000
AMOVA-Groupings	SSRs				AMOVA-Groupings	COI			
AMOVA2- two groups: NE Atlantic-West Med vs East Med	(Portuguese Waters East, Sardinian, Adventura e Maltese Bank) vs (Adriatic, Jonian, Levant)				AMOVA2- two groups: NE Atlantic-West Med vs East Med	(Portuguese Waters East, Sardinian, Adventura e Maltese Bank) vs (Adriatic, Jonian, Aegean, Levant)			
	Total variation (%)	<i>F</i> statistics		P		Total variation (%)	ϕ statistics		P
Among groups	60.6500	FCT	0.6065	0.0000+-0.0000	Among groups	32.0300	FCT	0.3203	0.0000+-0.0000
Among population within groups	7.9900	FSC	0.2029	0.0000+-0.0000	Among population within groups	35.0600	FSC	0.5157	0.0000+-0.0000
Within population	31.3600	FST	0.6864	0.0000+-0.0000	Within population	32.9200	FST	0.6708	0.0000+-0.0000
AMOVA-Groupings	SSRs				AMOVA-Groupings	COI			
AMOVA3-three groups belonging to the Atlantic Africa	(Middle Aghulas) vs (Cunene) vs (Cape Verde)				AMOVA3-three groups belonging to the Atlantic Africa	(Middle Aghulas) vs (Cunene) vs (Cape Verde)			
	Total variation (%)	<i>F</i> statistics		P		Total variation (%)	ϕ statistics		P
Among groups	11.4600	FCT	0.1146	0.3293+-0.0049	Among groups	57.1700	FCT	0.5717	0.1683+-0.0036
Among population within groups	7.1000	FSC	0.0802	0.1538+-0.0037	Among population within groups	-2.7000	FSC	-0.0630	0.6451+-0.0045
Within population	81.4400	FST	0.1857	0.0000+-0.0000	Within population	45.5200	FST	0.5448	0.0000+-0.0000

Table 9. Three-level AMOVA with three different groupings.

The parsimony network of the COI haplotypes in Fig.12 identified two main macro-haplogroups, coherently with the boundaries between geographical samples assessed by SSRs analysis. A clear differentiation between the Atlantic African and the NE Atlantic-Mediterranean samples was unequivocal.

Considering the South-Atlantic African haplogroup, it was characterized by shared haplotypes belonging to Middle Agulhas samples. The latter were separated by one mutation from the haplotype belonging to Cunene, while private haplotypes were observed in Cape Verde and Cunene divisions respectively.

A total of 16 mutations separated the African *R. miraletus* (ex. *R. ocellifera*) from the NE Atlantic-Mediterranean *R. miraletus* haplogroup. Among the latter, at a phylogeographical level, the largest haplotype was shared by a high number of individuals coming from both Western and Eastern Mediterranean Basin (FAO divisions: Balearic, Sardinia, Ionian, Adriatic) including Adventura and Maltese Bank.

Balearic and Sardinia divisions showed well-defined haplotypes within the largest Mediterranean haplogroup, while a smaller one reunited the Portuguese Waters, Balearic and Ionian divisions.

A third haplogroup embraced individuals of Eastern Mediterranean Basin (Ionian, Adriatic and Aegean divisions), including an unusually haplotype of Maltese Bank. Balearic and Ionian divisions shared a fourth haplotype, while two more haplotypes belonging to Levant area resulted independent.

Focusing on the NE Atlantic-Mediterranean haplogroup a slight differentiation was observed, a part of Balearic division and Ionian were the most frequent haplotypes, which appeared to be shared more than once within the Mediterranean haplogroup.

This pattern could be considered as a signal that the southern limit of Mediterranean continental shelf could fulfil the role of a continuous *couloir* connecting the westernmost part of the Basin to the centre-south (a part of Balearic, Sardinia and Ionian division). Similarly Ionian (JON/04), which appeared to be an admixed area when referring to the nuDNA signal, fell into the Algerian-Sicilian *couloir*. Splitting between the West and the East Mediterranean can be also seen considering the haplotypes. The most common haplotype (90 individuals) mainly embraced the samples of the West Mediterranean. The 62 individuals haplotype included the Adriatic samples and a two individuals from Greece. The 21 individuals haplotype incorporated a part of the Sicilian Channel samples, while the remaining part was shared between 31 individuals including the Portuguese and the two Algerian samples.

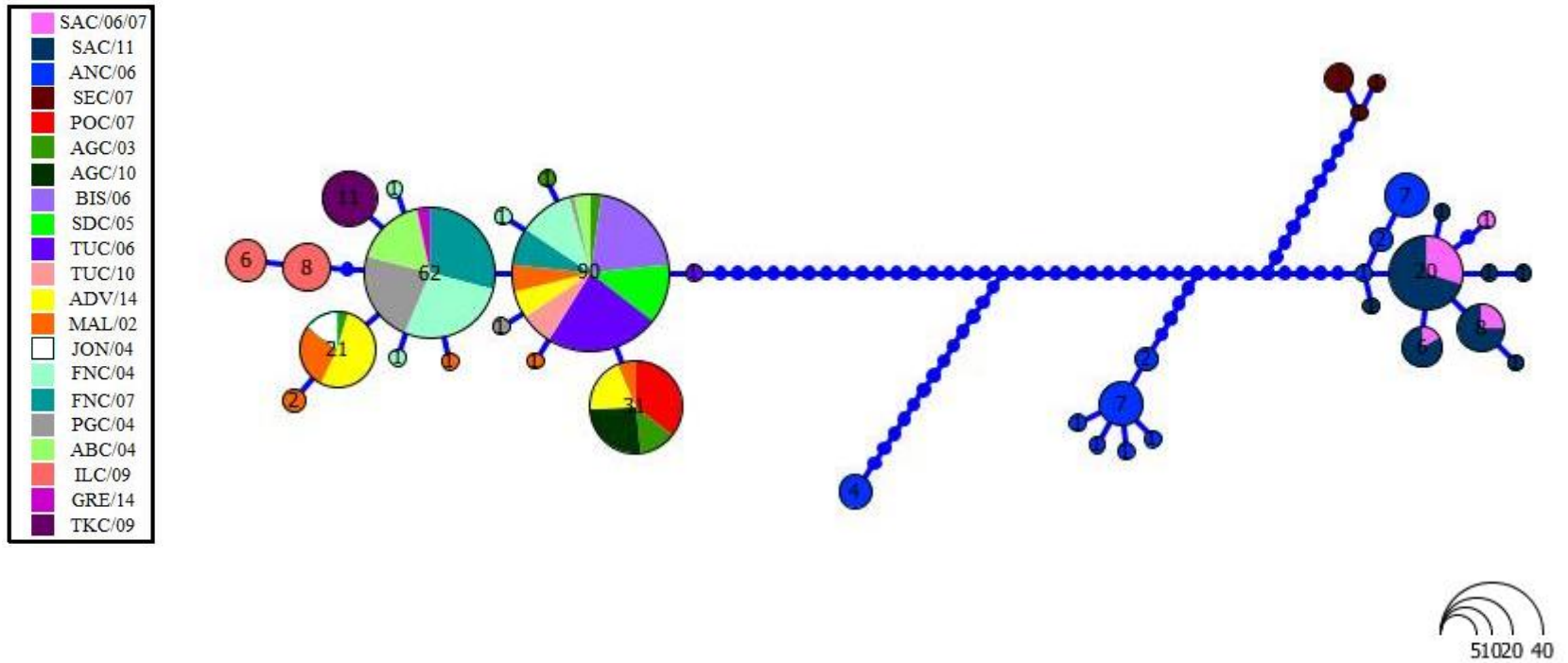


Figure 12. Statistical parsimony network of the COI haplotypes of Atlantic African and NE Atlantic-Mediterranean *Raja miraletus*. The confidence interval was at 95%. Numbers in circles represent the number of individuals that share a determinate haplotype. The size of the circles is proportional to the number of individuals that shared that haplotype. Refer to Tab.II for the distribution of the COI haplotypes among *R. miraletus* population samples.

The population structure of *R. miraletus* was also investigated with a Bayesian clustering analysis implemented in the software STRUCTURE and assessed with STRUCTURE Harvester, which identified K=3 and K=4 as the most appropriate K according to the Pritchard criterion considering the trend of LnP(K) (Fig.13a), while according to Evanno et al. (2005) the true value of K is K=2 (Fig.13b).

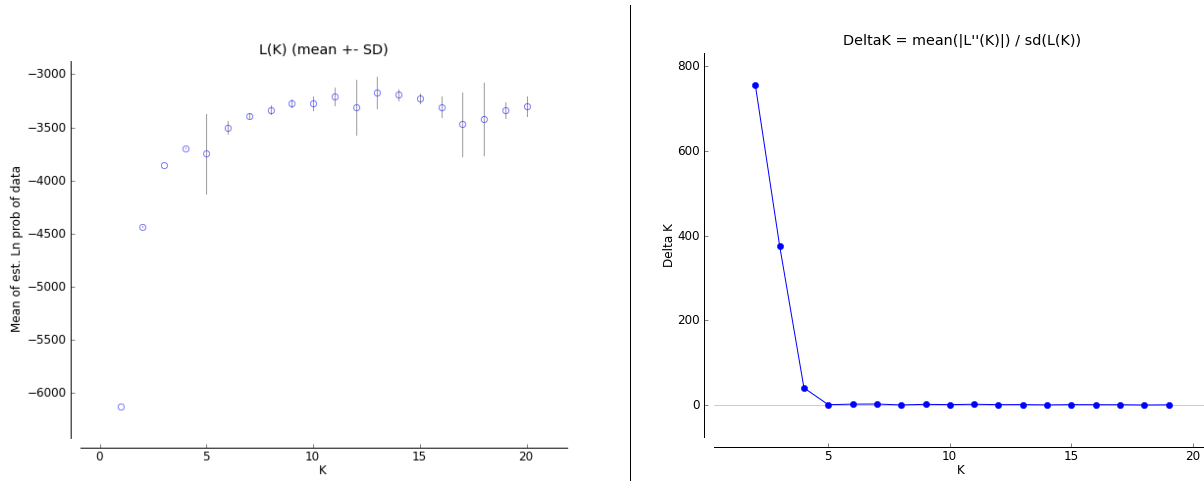


Figure 13a (left panel). Mean Ln(K). **Figure 13b (right panel).** Absolute value of ΔK .

Here I report clustering barplots for K=2, 3, 4 (Fig.14). With K=2 samples clearly divided into two main groups: Atlantic Africa and NE-Atlantic Mediterranean Sea. In particular, SEC/07 showed admixing genetic composition of the two clusters. With K=3 the clustering highlighted a deeper differentiation between Atlantic Africa, NE Atlantic-Western Mediterranean and Eastern Mediterranean samples. SEC/07 still showed similar admixing pattern as for K=2 and a new admixing area between the two Mediterranean clusters appeared for the sample JON/04. With K=4, ANC/06 showed a high level of admixture of two genetic components, one shared with SAC/11 and SAC/06 and the other belonging to SEC/07. The latter seemed to be completely independent, while the Western-Eastern Mediterranean subdivision remained mostly unvaried. Nevertheless, in light of the PCoA and AMOVA results, a deeper analysis was needed.

Therefore, the same analysis was coherently applied on a subset of 190 individuals, divided in 16 geographic samples, belonging to the NE Atlantic and Mediterranean samples.

STRUCTURE Harvester identified K=3, K=4 and K=5 as the most appropriate K according to the Pritchard criterion considering the trend of LnP(K) (Fig.15a), while according to Evanno et al. (2005) the true value of K is K=2 (Fig.15b). Here I report clustering barplots for K=2, 3, 4 and 5 (Fig.16).

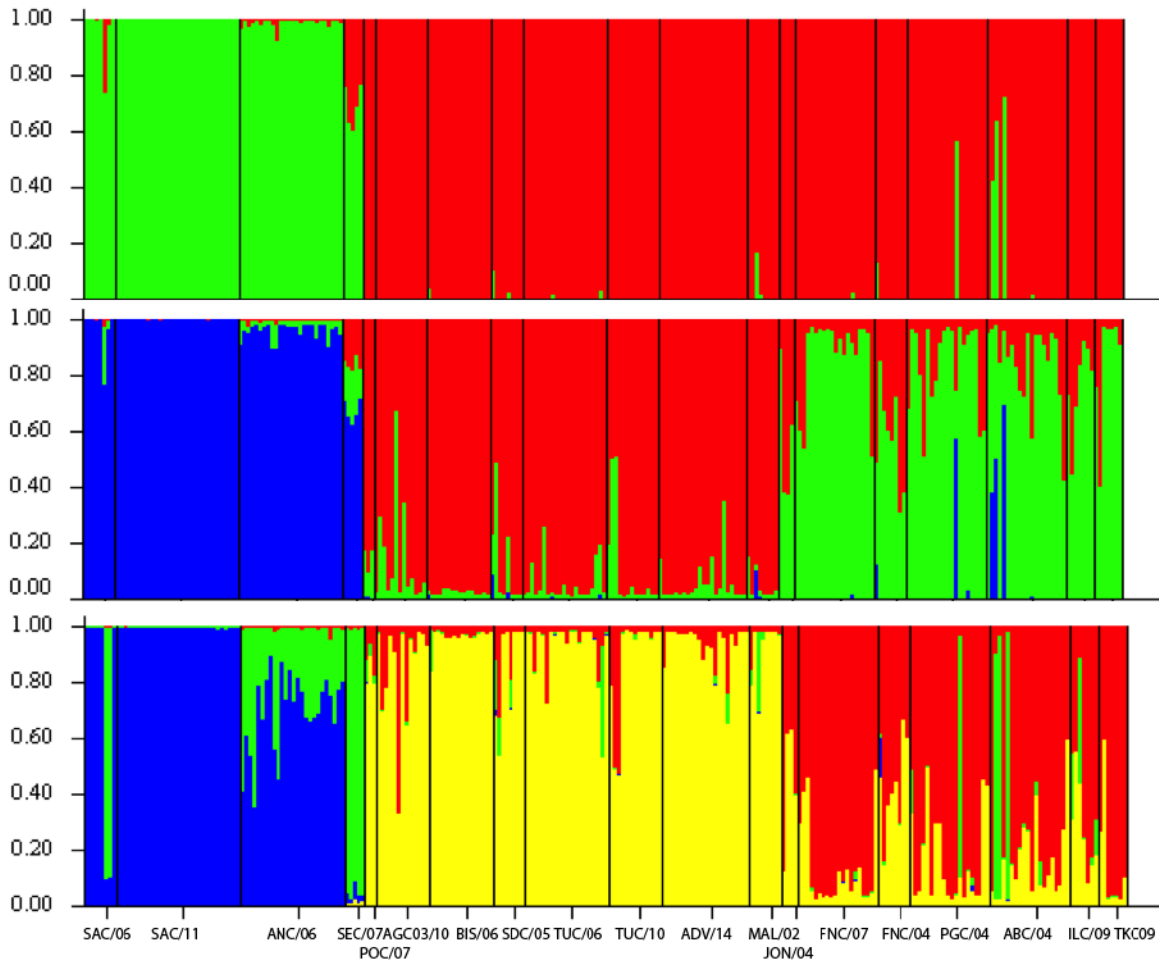


Figure 14. Bayesian assignment of *Raja miraletus* individuals built on the complete SSRs dataset and with estimated $K=2, 3, 4$. On the horizontal axis are reported the geographic samples, while on the vertical axis is reported the percentage of individual membership to a given genetic cluster. Single vertical bar represents one individual. Fractions of colour of a bar represent the estimated membership to a certain genetic group of that individual. Black lines separate different localities set *a priori*.

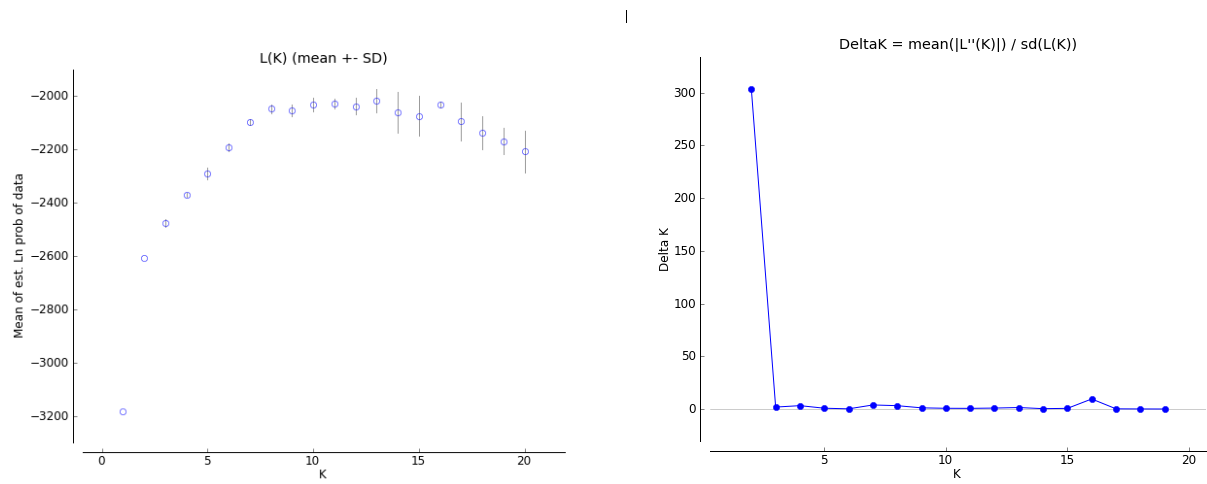


Figure 15a (left panel). Mean $\ln(K)$. **Figure 15b(right panel).** Absolute value of ΔK .

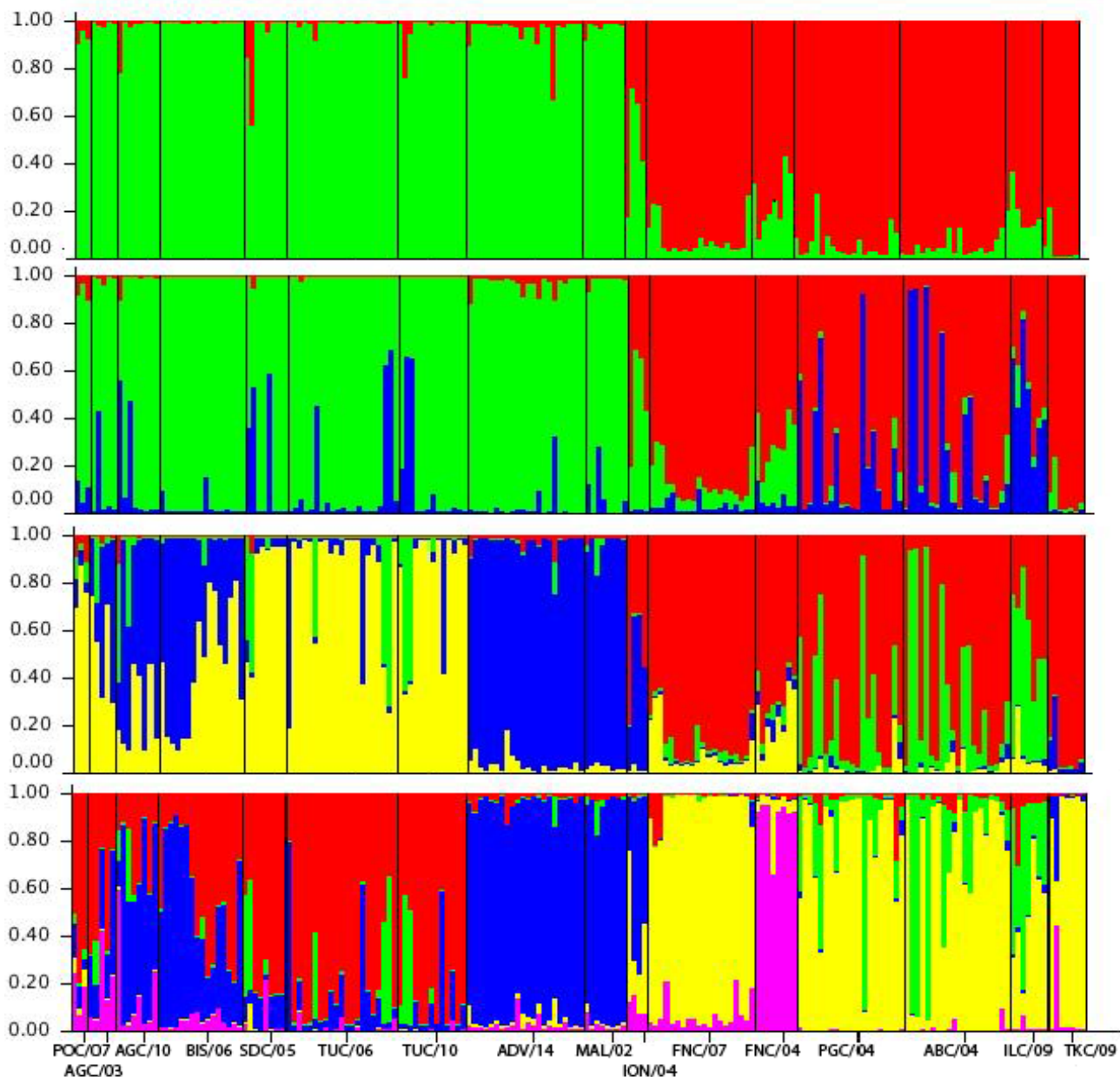


Figure 16 Bayesian assignment of *Raja miraletus* individuals built on the NE Atlantic-Mediterranean SSRs dataset and with estimated $K=2, 3, 4, 5$. On the horizontal axis are reported the geographic samples, while on the vertical axis is reported the percentage of individual membership to a given genetic cluster. Single vertical bar represents one individual. Fractions of colour of a bar represent the estimated membership to a certain genetic group of that individual. Black lines separate different localities set *a priori*.

For the clustering results obtained with $K=2$, no differences were highlighted in relation to what obtained over all samples with $K=3$ (Fig.14).

Results for $K=3$ showed that individuals belonged to two main genetic entities: NE Atlantic-Western Mediterranean (from POC/07 to MAL/02) and the second one of Eastern basin (from FNC/07 to TKC/09). ION/04 was confirmed to be an admixing area, while a third genetic component appeared scattered throughout the whole plot.

With $K=4$ a deeper structuring between samples of Western and Eastern localities started to appear. Within the Western Mediterranean group, Adventura and Maltese Bank individuals presented a different genetic

make-up in relation to Portuguese and Balearic samples, which also appeared different from those belonging to the Sardinian division. Within the Eastern Mediterranean group, the Bayesian assignment plot showed a main genetic entity, which was not reported among the Western Mediterranean populations.

Considering $K=5$ the strongest distinction between three main groups could be identified. In particular, samples belonging to NE Atlantic-Western Mediterranean (POC/07, AGC/03, AGC/10, BIS/06, SDC/05, TUC/06 and TUC/10) are clearly separated from the Sicilian Channel (ADV/14 and MAL/02), which, in turn, deeply recalled a certain genetic component found along the Algerian Coasts and around the Balearic Islands (AGC/03, AGC/10 and BIS/06). Then, the transitional area represented by JON/04 connected the Sicilian Channel with FAN/07, representing the Western Coasts of the Adriatic Sea. A strong differentiation and independent genetic composition was showed by FAN/04 corresponding instead to the Eastern Coasts of the Adriatic Sea. In closing, the Southern Adriatic Sea, Israelian coasts and Levantine Sea (PGC/04, ABC/04, ILC/09 and TKC/09) recalled the FAN/07 component, even if it appeared more scattered and admixed.

Differently, considering $K=5$ a distinction between three main groups could be identified. In particular, samples belonging to NE Atlantic-Western Mediterranean (POC/07, AGC/03, AGC/10, BIS/06, SDC/05, TUC/06 and TUC/10) are clearly separated from the Sicilian Channel (ADV/14 and MAL/02), which, in turn, recalled a certain genetic component found along the Algerian Coasts and around the Balearic Islands (AGC/03, AGC/10 and BIS/06).

Then, the transitional area represented by JON/04 connected the Sicilian Channel with FAN/07, representing the Western Coasts of the Adriatic Sea.

A strong differentiation and independent genetic composition was showed by FAN/04 corresponding instead to the Eastern Coasts of the Adriatic Sea.

3.4. Demographic history

The chronogram in Fig.17 reconstructed the Time of the Most Common Recent Ancestor (TMRCA) of the *R. miraletus* complex. Numbers near nodes represented the divergence time estimates expressed in MYA. The separation (posterior=1) between the out-group *R. asterias* and *R. miraletus* complex occurred 15.98MYA. The statistically supported node (posterior=1) for TMRCA of *R. miraletus* complex was estimated 11.74MYA. This period seemed to sign the differentiation between the Atlantic African (ex *R. ocellifera*) and the NE-Atlantic-Mediterranean *R. miraletus* species. The split between the Atlantic African haplotypes and the Angolan ones (Hap_12) occurred 10.34MYA. The separation from the Senegalese clade (Hap_20-22) from the South-Central African one occurred 4.48MYA, and within the latter where a further split dated 1.79MYA. The NE Atlantic-Mediterranean clade resulted as the most recent (1.91MYA), even if the separation between Eastern and Western Mediterranean did not appear clear. The TMRCA of Atlantic African (ex *R. ocellifera*) and the NE Atlantic-Mediterranean *R. miraletus* was estimated from the COI

dataset, supporting a recent divergence of those that we could define as siblings ex *R. ocellifera* and *R. miraletus*. This result was concordant with previous studies stating that the North-eastern Atlantic and Mediterranean skates diversified approximately from 17 to 1.8MYA (Valsecchi et al. 2005).

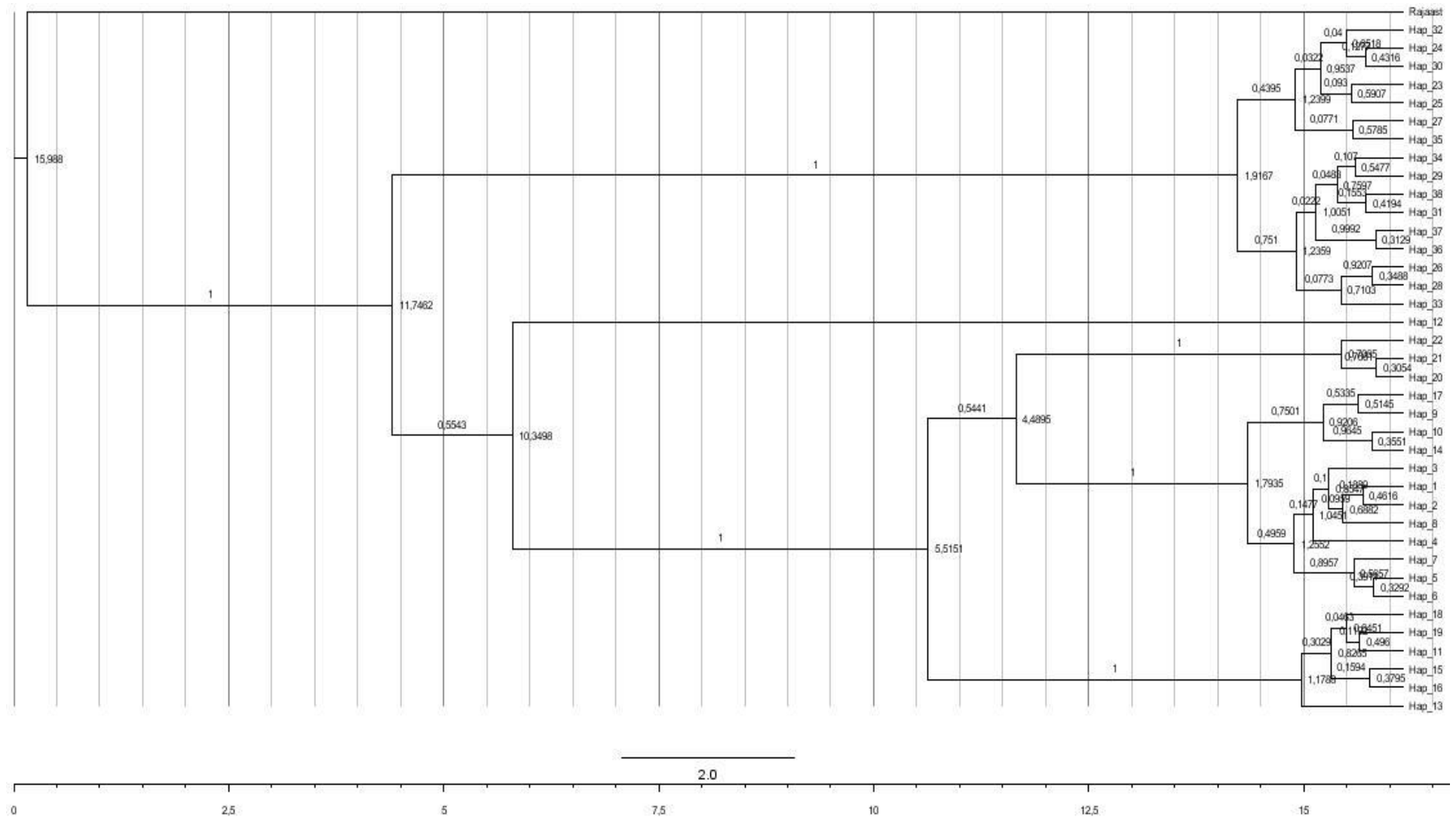


Figure 17. Chronogram illustrating the TMRCA of *Raja miraletus* complex. Refer to Tab.II for the distribution of the COI haplotypes among *R. miraletus* population samples. Numbers near nodes represent the divergence time in MY, while numbers along branches represent the posterior value of probability.

4. DISCUSSION AND CONCLUSIONS

The evolutionary history of skates has been described in recent times (Valsecchi et al. 2005; Chevolut et al. 2006; Compagno and Ebert, 2007; Tinti, 2008; Iglesias et al. 2009; Pasolini et al. 2011; Messinetti, 2013), but few and fragmented references focused on the Brown skate species complex (i.e. *Raja ocellifera* and *Raja miraletus*) proposed by McEachran et al. (1989) on the basis of morphometric variations among different geographical samples.

Considering the intrinsically sensitive ecological and biological traits and the scarce migratory behaviour of *R. miraletus*, the major impediment to its dispersal are the complex of oceanographic and hydrogeological discontinuities characterizing the Eastern Atlantic and the Mediterranean Basin. As a consequence, the past agreement about a uniform and contiguous marine realm seems more out-dated than ever. This thesis represents the final demonstration and identification of species boundaries in the *R. miraletus* complex on a wide geographical range, totally overlapping with the one considered in McEachran et al. (1989).

Following the wave of previous works by Ferrari (2012) and Vinjau (2012) I increased both nuDNA and mtDNA datasets with 19 additional individuals and other samples excluded from previous analyses (i.e. FAN/04 corresponding to the Croatian Coasts). The investigation based on both molecular markers, along with the merging and homogenization of previous fragmented information into a complete and exhaustive datasets, represents a first contribution to a wider aim. Taking advantage of the power of new analytical approaches in investigating genetic diversity, population differentiation and evolutionary backgrounds I analysed the merged datasets and I tested four main hypotheses regarding the Brown skate species boundaries along the African and NE Atlantic-Mediterranean Coasts, its phylogeography and demographic history.

In many cases, combining nuDNA and mtDNA markers improved the power of molecular data to test population structure and phylogeographic hypotheses and highlighted the incongruence of studies using only mtDNA rather than only nuDNA markers. As a matter of fact, in the past decade, many conflicting geographic patterns between mitochondrial and nuclear genetic markers have been identified (i.e. mito-nuclear discordance; Toews and Brelsford, 2012). In most cases, this incongruence is attributed to adaptive introgression of mtDNA, demographic disparities and sex-biased asymmetries, since the mitochondrial genome is haploid and uniparentally inherited in most animals. Given the ability for high-resolution nuclear genetic markers (i.e. microsatellites) to detect very slight and potentially very recent reductions in gene flow, it is becoming increasingly difficult to determine whether mtDNA homogeneity between groups, but divergent in nuDNA is a result of by male-biased dispersal, mating behaviour, sex-biased offspring production or of the high power of multi-locus nuclear data sets to detect differentiation (Edwards & Bensch 2009). In the present study, the combined analysis of nuDNA and mtDNA data indicated high levels of genetic diversity over all samples and the presence of at least two main clades characterized by different levels of connectivity within them.

Similarly to the findings based on morphometry and described in McEachran et al. (1989), a high variation, but slight/not significant differentiation were observed within the Atlantic African population (South Coast, Angola and Senegal (Tab.9), while the results of pair-wise Φ_{st} and F_{ST} have showed medium-high values of differentiation between Senegalese samples and the others. This result was supported by the high value of average genetic distance within the Atlantic African clade (0.0187) that probably defined a population differentiation *in actu*. Differently from the result within the Atlantic Africa, a deeper differentiation characterised the African and the NE Atlantic-Mediterranean populations and it was supported by multiple analyses as PCoA (Fig.8 and Fig.9), AMOVA (Tab.9), Haplotype network (Fig.12) and Bayesian individual assignment (Fig.14).

In first place, this work identified a speciation event between the Atlantic African clade, corresponding to the ex *R. ocellifera* nominal species, and the NE Atlantic-Mediterranean *R. miraletus* clade. The origin of this deep split dated 11.7MYA (Fig.17) and was likely due to the synergic influence of three main currents crossing the Western African Waters. Furthermore, the hypothetical effectiveness of the upwelling zones of Cape Blanco and Cape Frio in driving the evolution of the South-Eastern Atlantic skate fauna (Hulley, 1972; Briggs, 1974) was confirmed also for the Brown skate species complex. In particular, the Benguela Current flowing from Cape Agulhas to Cape Frio sustained the gene flow of ex *R. ocellifera* along the South Coast and Angolan shelf, up to the Angola-Benguela front. This would explain the shared genetic component characterizing individuals from SAC/06, SAC/11 and ANC/06 localities, but not the admixing of Angolan and Senegalese genetic clusters (Fig.14). In fact, the COI parsimony network in Fig.12 supports the total differentiation of the Senegalese sample (SEC/07) in relation to two Angolan haplotypes (ANC/06) through nine and 28 mutations respectively. The inter-tropical Canary Current inflowing from northeast likely influenced this pattern. This upper bound could have tackled the species gene flow across the North since its involvement in the development of an upwelling area around Cape Blanco. As a consequence, the most probable hydrogeographical barrier, responsible for the parapatric speciation between the sibling African (ex *R. ocellifera*) and the NE Atlantic-Mediterranean *R. miraletus* would be localized around Cape Blanco, in the Northern Mauritania. The allopatric and parapatric distribution of the *R. miraletus* complex was the result of past changes started with the closure of connection with Indian and Pacific Oceans.

A similar genetic architecture of the African mtDNA lineages was observed in Vinjau (2012), who detected a higher polymorphism over all loci, while a totally comparable spatial isolation among sibling species driven by geographical factors was observed by Pasolini et al. (2011), who dated the sibling *R. straeleni* and *R. clavata* TMRCA to the Early Pleistocene (1.3MYA), soon after the tumultuous palaeoclimatic history of equatorial and tropical Africa (Krueger et al. 2008).

If for the African population of ex *R. ocellifera* hydrogeographical breaks represented the trigger for a strong phylogeography and cryptic speciation, different/differently combined factors could have influenced the NE-Atlantic-Mediterranean clade.

Compared to other skate (Chevolot et al. 2005; Pasolini et al. 2011) and teleost species (Patarnello et al. 2007) no differentiation was observed between NE Atlantic and Mediterranean populations of *R. miraletus*. This led to suppose that the Strait of Gibraltar did not represent a barrier to gene flow, rather than an accession gate to ancient *refugia*.

At a smaller scale, the phylogeography and population structure indentified within the Basin seemed more linked to its particular bathymetry and a tighter relation with hydrogeological fronts or discontinuities.

According to nuDNA data, the most divergent geographical samples were Balearic (BIS/06), Sardinian (SDC/05, TUC/06, TUC/10), Ionian (ADV/14, MAL/02), and North-Eastern Adriatic (FNC/04) (Fig.15). As previously mentioned, the genetic component of ADV/14 and MAL/02 was detected among individuals belonging to Balearic populations (AGC/03, AGC/10 and BIS/06). This finding suggested in first place that the shallow bathymetry characterizing the Southwest part of the Basin would favour the transition of this bottom dwelling species.

In second instance, the rapid lowering of the seafloor level in correspondence of the edge between the easternmost part of Sicily (1000m) and the adjacent geo-morphological depression of the Calabrian Arc (3000m, corresponding to the deepest Ionian Sea) could have driven the differentiation of the Eastern Mediterranean Sea. In addition, this area is dominated from cyclonic/anti-cyclonic inversions of water masses. According to these observations this bathymetric and oceanographic discontinuity should have represented a barrier to gene flow and represented the Eastern bound letting to the Levantine's differentiation (Fig.12). On the contrary, the individual Bayesian clustering in Fig.16 showed the admixture of Western and Eastern genetic components characterizing precisely the Ionian population. The latter was considered a contact area, rather than a barrier, since traces of the Western genetic component was detected in South Adriatic division (PGC/04 and ABC/04), along the Israelian Coasts and easternmost Levantine. In this case mtDNA was more effective than the silent nuDNA in detecting genetic differentiations.

This strong population structure seemed to be peculiar of this species, whose ecological and biological traits are effective driving forces in shaping population boundaries.

Adults of *R. clavata*, for instance, display less restrictive habitat and depth preferences and a more pronounced migratory behaviour than the Brown skate (Serena, 2005) and did not show a similar deep differentiation when analysed at both nuclear-genomic and mtDNA markers (Chevolot et al. 2006; Bertucci Maresca, 2010; Pasolini et al. 2011).

The congeneric *R. polystigma*, endemic of Mediterranean and similar in size in relation to *R. miraletus*, occurred in the Western Basin as a panmictic unit with high levels of genetic diversity, with the exception of the Adriatic sample, characterized by a private COI haplotype (Frodella, 2012).

NuDNA analysis conducted on the Mediterranean *R. asterias* identified similar patterns as those observed in the Brown skate, since the Starry ray populations differentiated in three main groups: Western and Eastern Mediterranean Basins and Sicilian Channel.

The origin of the Mediterranean clade of *R. miraletus* obtained through the reconstruction of TMRCA indicated its recent origin during Pliocene (about 1.8MYA), when many geological events interested the

Mediterranean. Although it was not possible to recognize further signals of speciation within the Basin, two sub-clusters diversified approximately 1.2MYA. One clade included the Western Mediterranean haplotypes, while the second one showed shared haplotypes among Western and Eastern Mediterranean individuals. A clear and complete separation between these two parts of the Basins was not detected, since environmental and hydrogeographical factors might contribute to their dispersion and transition instead of tackle gene flow. The common tendency of skate fauna to suffer of reduced dispersal capacity contributed to their high genetic diversity and deep differentiation.

Furthermore, the high values of genetic variability observed in the most ancient species, *R. undulata* (Tab.8) could be considered a yardstick for the comparison of high distance values observed among the main Atlantic African and Mediterranean clades. With this result we could definitely confirm the occurrence of a speciation event between the Atlantic African clade (corresponding to the ex *R. ocellifera* nominal species) and the NE Atlantic-Mediterranean *R. miraletus* clade so defining *R. ocellifera* and *R. miraletus* two different species. These findings matched with previous studies on mtDNA and nuDNA markers used to measure the F_{ST} array observed between *R. clavata* and *R. straeleni* (Pasolini et al. 2011) and *R. polystigma* and *R. montagui* (Frodella, 2012). In conclusion, the *R. miraletus* species complex can be described as the as the most ancient cryptic speciation event of the family Rajidae, driven by the synergy of evolutionary and ecological forces on a wide geographical scale.

REFERENCES

- Abdulla, A., Gomei, M., Maison, E., Piante, C. (2008). Status of Marine Protected Areas in the Mediterranean Sea. Malaga, Spain: International Union for Conservation of Nature (IUCN); and France: World Wildlife Fund (WWF), pp. 152.
- Akaike, H. (1977). On entropy maximization principle. In Applications of Statistics, ed. P.R. Krishnaiah, North-Holland, Amsterdam, pp. 2741.
- Aschliman, N.C., Nishida, M., Miya, M., Inoue, J.G., Rosana, K.M., Naylor, G.J.P. (2012). Body plan convergence in the evolution of skates and rays (Chondrichthyes: Batoidea). Vol.63, pp. 28-42.
- Belkhir, K., Borsa, P., Chikhi, L., Raufaste, N., Bonhomme F. (2004). GENETIX 4.05, logiciel sous Windows TM pour la génétique des populations. Laboratoire Génome, Populations, Interactions, CNRS UMR 5171, Université de Montpellier II, Montpellier (France).
- Béranger, K., Mortier, L., Crépon, M. (2005). Seasonal variability of water transport through the Straits of Gibraltar, Sicily and Corsica, derived from a high resolution model of the Mediterranean circulation. Progress in Oceanography; Vol.66, pp. 341-364.
- Betroux, J. (1980). Mean water fluxes across sections in the Mediterranean Sea evaluated on the basis of water and salt budgets and of observed salinities. Oceanol. Vol.3, pp. 79-88.
- Bernardo, J. (2011). A critical appraisal of the meaning and diagnosability of cryptic evolutionary diversity, and its implications for conservation in the face of climate change. Cambridge University Press. The Systematics Association: Cambridge, UK, 2011.
- Bertucci Maresca, V. (2010). Phylogeography and Evolution of Mediterranean Elasmobranchs. Master Thesis, University of Trieste, Italy.
- Bianchi, C., Morri, C. (2000). Marine Biodiversity of the Mediterranean Sea: Situation, Problems and Prospects for Future Research. Marine Pollution Bulletin; Vol.40(5), pp. 367-376.
- Bickford, D., Lohman, D., Sodhi, N., Ng, P., Meier, R., Winker, K., Ingram, K., Das, I. (2007). Cryptic species as a window on diversity and conservation. Trends Ecology and Evolution. ScienceDirect; Vol.22 (3), pp. 148-155.
- Boero, F. (2003). State of Knowledge of Marine and Coastal Biodiversity in the Mediterranean Sea. Project for the Preparation of a Strategic Action Plan for the Conservation of Biological Diversity in the Mediterranean Region. (Sap BIO). Tunis: United Nations Environmental Programme, Regional Activity Centre for Specially Protected Areas, pp. 29.
- Briggs, J. (1974). Marine Zoogeography. McGraw-Hill book co., Inc., New York, pp. 475.
- Bryden, H.L., Candela, J., Kinder, T.H. (1994). Exchange through the Strait of the Gibraltar. Progress in Oceanography; Vol.33, pp. 201-248.
- Cadinu, M. (2009). Filogeografia e speciazione criptica di *Raja miraletus* (L. 1758). Master Thesis, University of Bologna, Italy.
- Cariani, A., Carlesi, L., Tosarelli, I., Serét, B., Tinti, F. (2010). Cryptic speciation and evolutionary history of the *Raja miraletus* species complex. In: Proceedings of the 14th European Elasmobranch Association Scientific Conference, Galway, Ireland, 10–13th November 2010. Irish Elasmobranch Group, pp. 18.

- Cariani, A., Ferrari, A., Tinti, F., Vinjau, S., the Elasmomed Consortium, Velonà, A. (2012). Parapatric cryptic speciation of *Raja miraletus* (L., 1758) species complex discovered from mitochondrial and nuclear markers. EEA 22-25 November 2012, Milan, pp. 97(Poster).
- Carvajal-Rodriguez, A., de Uña-Alvarez, J. (2011). Assessing Significance in High-Throughput Experiments by Sequential Goodness of Fit and q-Value Estimation. PLoS ONE; Vol.6(9) e24700.
- Chapuis, M., Estoup, A. (2007). Microsatellite null alleles and estimation of population differentiation. Mol. Biol. Evol; Vol.24(3), pp. 621-631.
- Chevolut, M., Reusch, T., Boele-Bos, S., Stam, W., Olsen, J. (2005). Characterization and isolation of DNA microsatellite primers in *Raja clavata* L. (thornback ray, Rajidae). Mol Ecol Notes; Vol.5, pp. 427-429.
- Chevolut, M., Hoarau, G., Rijnsdorp, A.D., Stam, W.T., Olsen, J.L. (2006). Phylogeography and population structure of thornback rays (*Raja clavata* L., Rajidae). Mol Ecol. Vol.15, pp. 3693-3705.
- Chevolut, M., Ellis, J., Hoarau, G., Rijnsdorp, A., Stam, W., Olsen, J. (2006a). Population structure of the thornback ray (*Raja clavata* L.) in British waters. J Sea Res; Vol.56, pp.305-316.
- Chevolut, M., Hoarau, G., Rijnsdorp, A., Stam, W., Olsen, J. (2006b). Phylogeography and population structure of thornback rays (*Raja clavata* L., Rajidae). Mol Ecol; Vol.15, pp. 3693-3705.
- Coll, M., Piroddi, C., Steenbeek, J., Kaschner, K., Ben Rais Lasram, F. (2010). The Biodiversity of the Mediterranean Sea: estimates, patterns, and threats. PLoS ONE. Vol.5(8).
- Compagno, L.J.V., Ebert, D., Smale, M.J. (1989). Guide to the sharks and rays of southern Africa. New Holland (Publ.) Ltd., London, pp. 158.
- Compagno, L.J.V., Ebert, D. (2007) Southern African skate biodiversity and distribution. Environ. Biol. Fish; Vol.80 (2), pp. 125-145.
- Dinieri, A. (2008). Accrescimento e composizione delle larve di acciuga (*engraulis encrasicolus*) in zone a diverse condizioni idrologiche del canale di Sicilia. Tesi di dottorato in Scienze Ambientali. Università Cà Foscari, Venezia.
- Drummond, A.J., Suchard, M.A., Xie, D., Rambaut, A (2012) Bayesian phylogenetics with BEAUti and the BEAST 1.7 Molecular Biology And Evolution; Vol.29, pp. 1969-1973.
- Earl, D., Von Holdt (2012). STRUCTURE HARVESTER: a website and program for visualizing STRUCTURE output and implementing the Evanno method. Conserv. Genet. Res.; Vol.4, pp. 359-361.
- Edwards, S.V., Bensch, S. (2009). Looking forwards or looking backwards in avian phylogeography? A comment on Zink and Barrowclough 2008. Molecular Ecology, Vol.18, pp. 2930–2933.
- El Nagar, A., McHugh, M., Rapp, T., Sims, D.W., Genner, M.J. (2010). Characterisation of polymorphic microsatellite markers for skates (Elasmobranchii: Rajidae) from expressed sequence tags. Conserv. Genet.; Vol.11, pp. 1203-1206.
- Evanno, G., Regnaut, S., Goudet, J. (2005). Detecting the number of clusters of individuals using the software Structure: A simulation study. Molecular Ecology; Vol. 4, pp. 2611-2620.
- Excoffier, L., Smouse, P., Quattro, J. (1992). Analysis of molecular variance inferred from metric distances among DNA haplotypes: application to human mitochondrial DNA restriction data. Genetics; Vol.131, pp. 479-91.

- Excoffier, L., Lischer, H. (2010) Arlequin suite ver 3.5: A new series of programs to perform population genetics analyses under Linux and Windows. *Molecular Ecology Resources*. Vol.10, pp. 564-567.
- Falush, D., Stephens, M., Pritchard, J.K. (2007) Inference of population structure using multilocus genotype data: linked loci and correlated allele frequencies. *Genetics*, Vol.164, pp. 1567-1587.
- Felsenstein, J. (2005). PHYLIP (Phylogeny Inference Package) version 3.6. Distributed by the author. Department of Genome Sciences, University of Washington, Seattle.
- Ferrari, A. (2012). Population structure and connectivity of the Mediterranean *Raja miraletus* (L. 1758). Master Thesis, University of Bologna, Italy.
- Froese and Pauly (2015). FishBase, World Wide Web electronic publication. www.fishbase.org. Version 02/2015.
- FAO (1990-2016). CWP Major Fishing Areas. CWP Data Collection. In: FAO Fisheries and Aquaculture Department [online]. Rome.
- Frodella, N. (2012). Conservation genetics of *Raja polystigma* (Regan, 1923): population structure, phylogeography and hybridization with the sibling parapatric species *Raja montagui* (Fowler, 1910). Master Thesis, University of Bologna, Italy.
- Galarza, J., Carreras-Carbonell, J., Macpherson, E., Pascual, M., Roques, S., Turner, G., Rico, C. (2009). The influence of oceanographic fronts and early-life-history traits on connectivity among littoral fish species. *PNAS*; Vol.106, pp. 1473-1478.
- García-Lafuente, J., García, A., Mazzola, S., Quintanilla, L., Delgado, A., Cuttitta, A., Patti, B. (2002). Hydrographic phenomena influencing early life stages of the Sicilian Channel anchovy. *Fisheries Oceanography*; Vol.11, pp. 31-44.
- Goudet, J. (2002). FSTAT, a program to estimate and test gene diversities and fixation indices (version 2.9.3.2). <http://www2.unil.ch/popgen/softwares/fstat.htm>.
- Griffiths, A.M., Sims, D.W., Cotterell, S.P., El Nagar, A.E., Ellis, J.R., Lynghammar, A., Mchugh, M., Neat, F.C., Pade, N.G., Queiroz, N., Serra-Pereira, B., Rapp, T., Wearmouth, V.J., Genner, M.J. (2010). Molecular markers reveal spatially-segregated cryptic species in a critically endangered fish, the common skate (*Dipturus batis*). *Proceedings of the Royal Society B-Biological Sciences*; Vol.277 (1687), pp. 1497-1503.
- Henderson, A.J., Reeve, R.W.J., Naylor G.J.P. (2015). Taxonomic assessment of sharks, rays and guitarfishes (Chondrichthyes: Elasmobranchii) from south-eastern Arabia, using the NADH dehydrogenase subunit 2 (NADH2) gene. *Zoological Journal of the Linnean Society*; Vol.176 (2), pp. 399-442.
- Hulley, P. (1972). The origin, interrelationships and distribution of southern african Rajidae (Chondrichthyes, Batoidei). *Annals of the South African Museum*; Vol.60 (1), pp. 1-103.
- Iglésias, S., Toulhoat, L., Sellos, D. (2009). Aquatic Conservation Marine Freshwater Ecosystem.
- Kalinowski, S., Wagner, A., Taper, M. (2006) ML-Relate: Software for estimating relatedness and relationship from multilocus genotypes. *Molecular Ecology Notes*; Vol.6, pp. 576-579.
- Krueger, S., Leuschner, D., Hermann, W., Schmiel, G., Mackenses, A., Diekmann, B. (2008). Ocean circulation patterns and dust supply into the South Atlantic during the last glacial cycle revealed by statistical analysis of kaolinite/chlorite ratios. *Mar. Geol.* Vol.253, pp. 82-91.

- Lermusiaux, P. (1998). Estimation and study of mesoscale variability in the Strait of Sicily. Dynamics of Atmospheres and Oceans (Special issue in honor of Professor A.R. Robinson); Vol.29, pp. 255-303.
- Lermusiaux, P., Robinson, A. (2001). Features of dominant mesoscale variability, circulation patterns and dynamics in the Strait of Sicily. Deep Sea Research I; Vol.48, pp. 1953-1997.
- Manzella, G., Gasparini, G., Astraldi, M. (1988). Water exchange between the Eastern and Western Mediterranean through the Strait of Sicily. Deep-Sea Res; Vol.35, pp. 1021-1035.
- McEachran, J.D., Seret, B., Miyake, T. (1989). Morphological variation within *Raja miraletus* and status of *Raja ocellifera* (Chondrichthyes: Rajoidei). Copeia, Vol.1989(3), pp. 629-641.
- McEachran, J., Dunn, K. (1998). Phylogenetic analysis of skates, a morphologically conservative clade of elasmobranchs (Chondrichthyes: Rajidae). Copeia; Vol (1998), pp. 271-290.
- Messinetti, S. (2013). Molecular phylogeny and historical zoogeography of four genera of Eastern Atlantic skates (Rajiformes, Rajidae). Master Thesis, University of Bologna, Italy.
- Moulton, M., Song, H., Whiting, W. (2010). Assessing the effects of primer specificity on eliminating numt coamplification in DNA barcoding: a case study from Orthoptera (Arthropoda: Insecta). Molecular Ecology; Vol.10, pp. 615–627.
- Mytilineou, C., Politou, C.Y., Papaconstantinou, C., Kavadas, S., D'Onghia, G., Sion, L. (2005). Deep-water fish fauna in the Eastern Ionian Sea. Belg. J. Zool; Vol.135(2), pp. 229-233.
- Nei, M. (1987). Molecular Evolutionary Genetics. Columbia University Press, New York, NY, USA.
- Ovenden, J.R., Morgan, J.A., Street, R. (2011). Negligible evidence for regional genetic population structure for two shark species *Rhizoprionodon acutus* (Rüppell, 1837) and *Sphyrna lewini* (Griffith & Smith, 1834) with contrasting biology. Marine Biology; Vol.158, pp. 1497-1509.
- Pasolini, P., Ragazzini, C., Zaccaro, Z., Cariani, A., Ferrara, G., Gonzalez, E.G., Landi, M., Milano, I., Stagioni, M., Guarniero, I., Tinti, F. (2011). Quaternary geographical sibling speciation and population structuring in the Eastern Atlantic skates (suborder Rajoidea) *Raja clavata* and *R. traeleni*. Marine Biology; Vol.158, pp. 2173-2186.
- Patarnello, T., Volckaert, F., Castilho, R. (2007). Pillars of Hercules: is the Atlantic-Mediterranean transition a phylogeographical break? Mol Ecol; Vol.16, pp. 4426-4444.
- Pavan-Kumar, P., Gireesh-Babu, P.P., Suresh Babu, A.K., Jaiswar, K., Pani, P., Aparna Chaudhari, S.G., Raje, S.K., Chakraborty, G.K., Lakra, W.S. (2013). DNA barcoding of elasmobranchs from Indian Coast and its reliability in delineating geographically widespread specimens. Mitochondrial DNA; Vol.26, pp. 92-100.
- Peakall, R., Smouse, P. (2012). GenAlEx 6.5: genetic analysis in Excel. Population genetic software for teaching and research – an update. Bioinformatics; Vol.28, pp. 2537-2539.
- Plank, S., Lowe, C., Feldheim, K., Wilson, R.R. Jr., Brusslan, J. (2010). Population genetic structure of the round stingray *Urobatis halleri* (Elasmobranchii: Rajiformes) in southern California and the Gulf of California. J Fish Biol. Vol.77, pp. 329-340.
- Pritchard, J.K., Stephens, M., Donnelly, P. (2000). Inference of population structure using multilocus genotype data. Genetics Vol.155, pp. 945-959.
- Quattro, J.M., Stoner, D.S., Driggers, W.B., Anderson, C.A., Priede, K.A., Hoppmann, E.C., Campbell, N.H. (2006). Genetic evidence of cryptic speciation within hammerhead sharks (Genus *Sphyrna*). Mar Biol; Vol.148, pp. 1143-55.

- Quinteiro, J., Rodriguez-Castro, J., Rey-Méndez, M. (2007). Population genetic structure of the stalked barnacle *Pollicipes pollicipes* (Gmelin, 1789) in the northeastern Atlantic: influence of coastal currents and mesoscale structures. *Mar. Biol.*; Vol.153, pp. 47-60.
- Regan, C. (1906). Description of new or little know fishes from the coast of Natal. *Ann Natal Gov. Mus.*; Vol.1(1), pp. 1-6.
- Rice, W.R. (1989). Analyzing tables of statistical tests. *Evolution*; Vol.43, pp. 223-225.
- Robinson, A., Sellschopp, J., Warn-Varnas, A., Leslie, W., Lozano, C., Haley, P., Anderson, L., Lermusiaux, P. (1999). The Atlantic Ionian Stream. *Journal of Marine Systems*; Vol.20, pp. 113-128.
- Rousset, F. (2008). Genepop'007: a complete reimplementation of the Genepop software for Windows and Linux. *Mol. Ecol. Resources*; Vol.8, pp. 103-106.
- Rozas, J., Librado, P. (2009). DnaSP v5: a software for comprehensive analysis of DNA polymorphism data. *Bioinformatics*; Vol.25, pp. 1451-1452.
- Sandoval-Castillo, J.R., Rocha-Olivares, A., Villavicencio Garayzar, C., Balart, E. (2004). Cryptic isolation of Gulf of California shovelnose guitarfish evidenced by mitochondrial DNA. *Mar Biol*; Vol.145, pp. 983-988.
- Serena, F. (2005). Field identification guide to the sharks and rays of the Mediterranean and Black sea. FAO species identification guide for fishery purposes. Roma, pp. 62-66.
- Serra-Pereira, B., Moura, T., Griffiths, A.M., Serrano Gordo, L., Figueiredo, Y. (2010). Molecular barcoding of skates (Chondrichthyes: Rajidae) from the southern Northeast Atlantic. *Zoologica Scripta*; Vol.40 pp. 76-84.
- Shirai, S. (1996). Phylogenetic interrelationships of neoselachians (Chondrichthyes, Euselachii). In *Interrelationships of fishes* (Stiassny, M.L.J., Parenti, R., Jhonson, G.D., eds). Academic Press, San Diego, USA and London, UK, pp. 9-34.
- Smale, M.J., Ungaro, N., Serena, F., Dulvy, N., Tinti, F., Bertozzi, M., Mancusi, C., Noarbartolo di Sciara G. (2009). *Raja miraletus*. In: IUCN 2011. IUCN Red List of Threatened Species. Version 2011.2. <http://www.iucnredlist.org> Downloaded on 02 March 2012.
- Stehmann, M., Bürkel, D.L. (1984). Rajidae. In: P.J.P. Whitehead, M.-L. Bauchot, J.-C. Hureau, J. Nielsen and E. Tortonese (eds.) *Fishes of the North-eastern Atlantic and the Mediterranean*. UNESCO, Paris; Vol.1, pp. 163-196.
- Tamura, K., Stecher, G., Peterson, D., Filipski, A., Kumar, S. (2013). Mega6: Molecular Evolutionary Genetics Analysis version 6.0. *Mol Biol Evol*; Vol.30, pp. 2725–2729.
- Thompson, J., Higgins, D., Gibson, T. (1994). CLUSTAL W: improving the sensitivity of progressive multiple sequence alignment through sequence weighting, position-specific gap penalties and weight matrix choice. *Nucleic Acids Res*; Vol.22(22), pp. 4673-80.
- Tinti, F. (2008). *Dispense di zoologia marina e biotecnologie marine*. University of Bologna, Italy.
- Toews, D.P.L., Brelsford, A. (2012). The biogeography of mitochondrial and nuclear discordance in animals. *Molecular Ecology* Vol.21(16), pp. 3907-3930.
- Tsimplis, M., Bryden, H. (2000). Estimation of the transport trough the Strait of the Gibraltar. *Deep-sea Research I*; Vol.47, pp. 2219-2242.

Valsecchi, E., Pasolini, P., Bertozzi, M., Garoia, F., Ungaro, N., Vacchi, M., Sabelli, B., Tinti, F. (2005) Rapid Miocene-Pliocene dispersal and evolution of Mediterranean rajid fauna as inferred by mitochondrial gene variation. *Journal of Evolutionary Biology*; Vol.18, pp. 436-446.

Vinjau, S. (2012). Phylogeography and population structure of the African *Rajamiraletus* (L., 1785) and *Leucoraja wallacei* (Hulley, 1970). Master Thesis. University of Bologna, Italy.

Wallace, J. H. 1967. The batoid fishes of the east coast of southern Africa. Part III: Skates and electric rays. *South African Assoc. Mar. Biol. Res. In-vest. Rept.* Vol.17, pp. 1-62.

Warn-Varnas, A., Sellschopp, J., Haley, P.J. Jr., Leslie, W.G., Lozano C.J. (1999). Strait of Sicily Water Masses. *Dynamics of Atmospheres and Oceans* (Special issue in honor of Professor A.R.Robinson); Vol.29, pp. 437-469.

APPENDIX

Locus name		Primer sequence (5' – 3')	Label	Core
Leri24	F	GCACGTACGCAGAATTTGAA	VIC	(TC)8
	R	CCGGCACGTGTAATTTAAGG		
Leri26	F	GCAGCAGCAGTGAGGACAAT	6-FAM	(GA)12
	R	CTCCTACCGTCATGCCTCAT		
Leri27	F	AACTGGGCAACTGACCACA	NED	(CT)15
	R	AACGTTCTGGGTGCTGCTAC		
Leri34	F	CTTGCAATCTTTTGCCGAGT	PET	(GT)11
	R	GTTTCATCGGCCTCTTGATGT		
Leri40	F	TGCTGTTTTAATGGCTTGTGA	NED	(TA)11
	R	TTCAGAAGGGCTTCCCATAA		
Leri44	F	CAGCGAGTAAACACCGACCT	6-FAM	(GT)11
	R	TGCGATGATCTTGAAAGACG		
Leri50	F	AATAATTGTGCCTCTTTGAGACAT	PET	(TA)11
	R	CACAGGGAACGCAATACCTT		
Leri63	F	TTTTGATCGGCTGCAAAAAT	VIC	(TC)8
	R	CGGACTGTATAATGTGTACCAACC		

Table2. Details of SSR loci used in this study (El Nagar et al. 2010)

Name	Ratio	Cocktail name/Primer sequence 5'–3' Product	Primer position	References
COI-3		C_FishF1t1–C_FishR1t1		
VF2_t1	1	TGTA AAAACGACGGCCAGTCAACCAACCACAAAGACATTGGCAC	6448–6474	*Ward et al. 2005 FishF2_t1 1
FishF2_t1	1	TGTA AAAACGACGGCCAGTCGACTAATCATAAAGATATCGGCAC	6448–6474	*Ward et al. 2005 FishR2_t1 1
FishR2_t1	1	CAGGAAACAGCTATGACACTTCAGGGTGACCGAAGAATCAGAA	7152–7127	*Ward et al. 2005 FR1d_t1 1
FR1d_t1	1	CAGGAAACAGCTATGACACCTCAGGGTGTCCGAARAAYCARAA	7152–7127	This study
M13F (–21)		TGTA AAAACGACGGCCAGT		Messing (1983)
M13F (–27)		CAGGAAACAGCTATGAC		Messing (1983)

Table 3. Details of primer cocktail designed for COI gene by Ivanova et al. (2007).

Table Ia. Allele frequencies per locus per population; N= number of analyzed individuals per locus per population.

Locus	SAMPLES																			
	SAC/07 N=8	SAC/11 N=31	ANC/06 N=26	SEC/07 N=5	POC/07 N=3	AGC/03 N=5	AGC/10 N=8	BIS/06 N=16	SDC/05 N=8	TUC/06 N=21	TUC/10 N=13	ADV/14 N=22	MAL/02 N=8	JON/04 N=4	FNC/04 N=8	FNC/07 N=20	PGC/04 N=20	ABC/04 N=20	ILC/09 N=7	TKC/09 N=7
Leri27																				
(N)	8	27	25	4	3	5	6	16	8	20	11	22	7	4	8	18	19	18	7	7
197	0.0868																			
201	0.0868		0.8000										0.7140				0.5260			
203			0.8000																0.2780	
205										0.4550									0.5560	
207			0.8000			0.1000		0.3130		0.5000		0.2270			0.6250					
209			0.6000						0.6250	0.2500		0.2270		0.7500		0.7500	0.7895	0.6667	0.8571	0.8571
211		0.1850	0.1200	0.1250	0.3333	0.9000	0.5000	0.1250	0.1250	0.2750	0.3182			0.2500	0.5625	0.2500	0.1316	0.2222	0.1429	0.1429
213	0.1250		0.1200	0.1250	0.6667		0.2500	0.8438	0.4375	0.6250	0.5990	0.6136	0.7143		0.1875			0.2780		
215	0.5000	0.7370	0.1200	0.2500			0.2500		0.3750	0.2500	0.4550	0.4550	0.2143		0.1875		0.2630			
217		0.1111	0.6000									0.2500								
219	0.1250	0.1111	0.4000									0.4550								
221			0.4000	0.1250																
223		0.5560	0.1400	0.1250																
225			0.4000	0.1250																
229			0.2000	0.1250																
SAMPLES																				
	SAC/07 N=8	SAC/11 N=31	ANC/06 N=26	SEC/07 N=5	POC/07 N=3	AGC/03 N=5	AGC/10 N=8	BIS/06 N=16	SDC/05 N=8	TUC/06 N=21	TUC/10 N=13	ADV/14 N=22	MAL/02 N=8	JON/04 N=4	FNC/04 N=8	FNC/07 N=20	PGC/04 N=20	ABC/04 N=20	ILC/09 N=7	TKC/09 N=7
Leri26																				
(N)	7	29	24	5	3	5	8	16	7	20	13	21	8	4	8	20	20	20	7	7
126				0.2000	1.0000	1.0000	0.8750	0.8750	0.8571	0.9000	0.9231	1.0000	1.0000	0.2500	0.3125	0.7500	0.1250	0.1000	0.2143	
128	0.2857	0.8620	0.5280						0.1429										0.7500	
130															0.1250	0.2500		0.5000		
136		0.5170		0.4000			0.1250	0.1250		0.7500	0.3850							0.1250		
138	0.2857	0.3130	0.8330	0.1000																
140	0.7140	0.4138	0.6250												0.1250					
142	0.2857	0.1340	0.1250																	
144			0.2800																	
146	0.7140	0.3450	0.4170							0.2500	0.3850			0.7500	0.3125				0.7140	0.1429
148			0.6250	0.3000											0.1250	0.9000	0.8750	0.6500	0.7143	0.8571
152			0.2800																	
154			0.6250																	

SAMPLES

	SAC/07	SAC/11	ANC/06	SEC/07	POC/07	AGC/03	AGC/10	BIS/06	SDC/05	TUC/06	TUC/10	ADV/14	MAL/02	JON/04	FNC/04	FNC/07	PGC/04	ABC/04	ILC/09	TKC/09
	N=8	N=31	N=26	N=5	N=3	N=5	N=8	N=16	N=8	N=21	N=13	N=22	N=8	N=4	N=8	N=20	N=20	N=20	N=7	N=7
Leri24																				
(N)	7	31	25	5	3	4	6	15	8	19	12	22	8	4	8	19	18	19	7	7
254	0.5714	0.6613	0.3200																	
256		0.1610	0.2600																	
258			0.4000																0.1530	
260	0.2857	0.3226	0.2400													0.2630			0.5260	
262			0.2000																	
264	0.1429		0.6000						0.1250						0.3750		0.4211	0.6111	0.2150	0.5714
266			0.2000			0.1250	0.3333	0.3667		0.7890	0.4170				0.3750				0.7140	
268			0.4000	0.2000	0.3333	0.7500	0.6667	0.5000	0.2500	0.5526	0.5417	0.6136	0.7500	0.2500	0.5625	0.5000	0.1667	0.6530	0.6429	0.4286
270						0.1250		0.3330	0.6250	0.3684	0.3750	0.3864	0.2500		0.4375		0.1667	0.2630	0.2857	
272				0.4000	0.3333			0.1000			0.4170									
274				0.3000	0.3333											0.5260	0.5560			
277				0.1000																

SAMPLES

	SAC/07	SAC/11	ANC/06	SEC/07	POC/07	AGC/03	AGC/10	BIS/06	SDC/05	TUC/06	TUC/10	ADV/14	MAL/02	JON/04	FNC/04	FNC/07	PGC/04	ABC/04	ILC/09	TKC/09
	N=8	N=31	N=26	N=5	N=3	N=5	N=8	N=16	N=8	N=21	N=13	N=22	N=8	N=4	N=8	N=20	N=20	N=20	N=7	N=7
Leri34																				
(N)	8	30	26	5	1	5	6	15	8	20	12	22	8	4	8	19	18	18	7	7
269		0.1670																		
273																			0.8330	
275	0.1250				1.0000	0.2000	0.5000	0.4667	0.1250	0.2500		0.2727	0.6250	0.6250	1.0000	0.8947	0.6667	0.7222	0.5714	0.7143
277		0.5000	0.3850			0.8000	0.5000	0.5333	0.7500	0.8500	1.0000	0.7273	0.8125	0.3750		0.1530	0.2778	0.1944	0.4286	0.2857
279	0.6875	0.5167	0.3846	0.2000					0.1250	0.1250			0.6250				0.5560			
281	0.1875	0.4167	0.4231	0.2000									0.6250							
283			0.1154	0.6000																
285			0.3850																	

SAMPLES

	SAC/07	SAC/11	ANC/06	SEC/07	POC/07	AGC/03	AGC/10	BIS/06	SDC/05	TUC/06	TUC/10	ADV/14	MAL/02	JON/04	FNC/04	FNC/07	PGC/04	ABC/04	ILC/09	TKC/09	
	N=8	N=31	N=26	N=5	N=3	N=5	N=8	N=16	N=8	N=21	N=13	N=22	N=8	N=4	N=8	N=20	N=20	N=20	N=7	N=7	
Leri63																					
(N)	7	31	26	5	3	4	6	16	7	14	13	22	7	3	8	17	19	19	4	7	
279	0.1429																				
283			0.3850																		
289			0.1920																		
291	0.5000	0.6613	0.3770																0.5260		
293			0.1731																0.5260		
297	0.2143	0.3387	0.2115																0.5260		
301			0.5770									0.6820		0.5000		0.3529	0.3158	0.2632	0.2632	0.1250	0.2857
303			0.7690						0.1429	0.1710					0.5625	0.1765	0.2632	0.5260		0.1429	
305	0.1429		0.1154	0.2000			0.7500	0.4630		0.1710	0.3850	0.5455	0.7143	0.5000		0.8820	0.7890	0.2630		0.3571	
307				0.1000	1.0000	1.0000	0.2500	0.5938	0.8571	0.7857	0.8846	0.3864	0.2857		0.4375	0.3824	0.2895	0.3421	0.7500	0.2143	
309				0.4000							0.7690						0.5260	0.1579	0.1250		
311				0.1000																	
313				0.1000																	
314				0.1000																	

SAMPLES

	SAC/07	SAC/11	ANC/06	SEC/07	POC/07	AGC/03	AGC/10	BIS/06	SDC/05	TUC/06	TUC/10	ADV/14	MAL/02	JON/04	FNC/04	FNC/07	PGC/04	ABC/04	ILC/09	TKC/09
	N=8	N=31	N=26	N=5	N=3	N=5	N=8	N=16	N=8	N=21	N=13	N=22	N=8	N=4	N=8	N=20	N=20	N=20	N=7	N=7
Leri50																				
(N)	8	30	26	4	3	5	7	14	6	18	13	22	8	4	8	16	14	15	5	7
312	0.1250	0.1670	0.3850	0.1250						0.5560										
314	0.7500	0.9833	0.9423	0.6250													0.7140	0.3330		
316			0.1920	0.2500																
318									0.8330									0.1333	0.5000	
320	0.1250				0.6667	0.6000	0.5714	0.5000	0.9167	0.4444	0.3846	1.0000	1.0000	1.0000	1.0000	0.6875	0.5714	0.6667	0.1000	0.6429
322					0.1667	0.2000	0.1429				0.2380					0.1250	0.3571	0.1000	0.2000	0.3571
324					0.1667	0.2000	0.2857	0.4286		0.4444	0.3846					0.1875		0.6670	0.2000	
326								0.7140		0.5560										

SAMPLES																				
	SAC/07	SAC/11	ANC/06	SEC/07	POC/07	AGC/03	AGC/10	BIS/06	SDC/05	TUC/06	TUC/10	ADV/14	MAL/02	JON/04	FNC/04	FNC/07	PGC/04	ABC/04	ILC/09	TKC/09
	N=8	N=31	N=26	N=5	N=3	N=5	N=8	N=16	N=8	N=21	N=13	N=22	N=8	N=4	N=8	N=20	N=20	N=20	N=7	N=7
Leri40																				
(N)	7	31	26	5	3	4	8	15	6	19	13	22	7	4	8	18	19	17	4	7
254	0.3571	0.1610	0.1154	0.4000				0.6670												
256	0.6429	0.9839	0.8846	0.6000																
258																			0.2940	
262								0.8330										0.1176	0.6250	
264					1.0000	1.0000	0.8125	0.9333	0.9167	0.8421	0.8462	1.0000	0.8571	1.0000	1.0000	0.8889	0.7368	0.7590	0.2500	0.9286
266							0.1875			0.1579	0.1538					0.1111	0.2150	0.1471	0.1250	0.7140
270													0.1429							
274																	0.5260			
SAMPLES																				
	SAC/07	SAC/11	ANC/06	SEC/07	POC/07	AGC/03	AGC/10	BIS/06	SDC/05	TUC/06	TUC/10	ADV/14	MAL/02	JON/04	FNC/04	FNC/07	PGC/04	ABC/04	ILC/09	TKC/09
	N=8	N=31	N=26	N=5	N=3	N=5	N=8	N=16	N=8	N=21	N=13	N=22	N=8	N=4	N=8	N=20	N=20	N=20	N=7	N=7
Leri44																				
(N)	4	16	12	2	1	3	7	16	6	21	12	21	8	4	8	16	17	16	5	5
277	0.7500	0.9688	1.0000																	
279		0.3130																		
283	0.1250																			
287																			0.3130	
289																			0.6250	
291												0.7140								
293				0.5000		0.1667	0.4286					0.7140	0.2500		0.6250			0.6250		
295												0.2380	0.6250							
297	0.1250						0.2143					0.2380	0.6250				0.5880	0.3130	0.1000	
299				0.5000	1.0000	0.5000	0.1429	1.0000	1.0000	1.0000	1.0000	0.6950	0.5000	0.7500	0.2500	0.3125	0.5588	0.2500	0.6000	
301						0.3333	0.2143					0.9520	0.6250	0.2500	0.6875	0.6563	0.2941	0.5000	0.1000	1.0000
303												0.2380						0.3130	0.2000	
305													0.6250							
307																0.3130	0.8820	0.3130		

Leri50																				
N	8.0000	30.0000	26.0000	4.0000	3.0000	5.0000	7.0000	14.0000	6.0000	18.0000	13.0000	22.0000	8.0000	4.0000	8.0000	16.0000	14.0000	15.0000	5.0000	7.0000
A	3.0000	2.0000	3.0000	3.0000	3.0000	3.0000	3.0000	3.0000	2.0000	4.0000	3.0000	1.0000	1.0000	1.0000	1.0000	3.0000	3.0000	5.0000	4.0000	2.0000
Ar	1.4330	1.0330	1.1120	1.6070	1.6000	1.6220	1.6150	1.5820	1.1670	1.6160	1.6770	1.0000	1.0000	1.0000	1.0000	1.4920	1.5610	1.5400	1.7330	1.4950
H _O	0.2500	0.0333	0.1154	0.7500	0.3333	0.0000	0.0000	0.0000	0.1667	0.0000	0.0000	0.0000	0.0000	0.0000	0.0000	0.0000	0.0000	0.1333	0.2000	0.1429
H _E	0.4063	0.0328	0.1102	0.5313	0.5000	0.5600	0.5714	0.5612	0.1528	0.5988	0.6509	0.0000	0.0000	0.0000	0.0000	0.4766	0.5408	0.5222	0.6600	0.4592
FIS	0.4400	0.0000	-0.0270	-0.2860	0.5000	1.0000	1.0000	1.0000	0.0000	1.0000	1.0000	NA	NA	NA	NA	1.0000	1.0000	0.7600	0.7500	0.7270
NA	0.1465	0.0001	0.0000	0.0000	0.0008	0.3659	0.3687	0.3615	0.0000	0.3766	0.3948	0.0010	0.0010	0.0010	0.0010	0.3371	0.3552	0.2580	0.2863	0.2222
HWE	0.1449	-	1.0000	1.0000	0.1930	0.0173*	0.0035*	0.0000*	-	0.0000*	0.0000*	-	-	-	-	0.0000*	0.0000*	0.0000*	0.016*	0.1051
Leri40																				
N	7.0000	31.0000	26.0000	5.0000	3.0000	4.0000	8.0000	15.0000	6.0000	19.0000	13.0000	22.0000	7.0000	4.0000	8.0000	18.0000	19.0000	17.0000	4.0000	7.0000
A	2.0000	2.0000	2.0000	2.0000	1.0000	1.0000	2.0000	2.0000	2.0000	2.0000	2.0000	1.0000	2.0000	1.0000	1.0000	2.0000	3.0000	4.0000	3.0000	2.0000
Ar	1.4950	1.0320	1.2080	1.5330	1.0000	1.0000	1.3250	1.1290	1.1670	1.2730	1.2710	1.0000	1.2640	1.0000	1.0000	1.2030	1.4210	1.4800	1.6070	1.1430
H _O	0.1429	0.0323	0.0769	0.8000	0.0000	0.0000	0.1250	0.0000	0.1667	0.0000	0.0000	0.0000	0.0000	0.0000	0.0000	0.0000	0.0000	0.1176	0.5000	0.1429
H _E	0.4592	0.0317	0.2041	0.4800	0.0000	0.0000	0.3047	0.1244	0.1528	0.2659	0.2604	0.0000	0.2449	0.0000	0.0000	0.1975	0.4100	0.4654	0.5313	0.1327
FIS	0.7270	0.0000	0.6350	-0.6000	NA	NA	0.6320	1.0000	0.0000	1.0000	1.0000	NA	1.0000	NA	NA	1.0000	1.0000	0.7600	0.2000	0.0000
NA	0.1677	0.0001	0.1469	0.0000	0.0010	0.0010	0.1641	0.1703	0.0000	0.2460	0.2435	0.0010	0.2364	0.0010	0.0010	0.2131	0.3100	0.2392	0.0000	0.0000
HWE	0.1068	-	0.017*	0.4300	-	-	0.1988	0.0341*	-	0.0004*	0.005*	-	0.0750	-	-	0.0026*	0.0000*	0.0000*	0.4246	-
Leri44																				
N	4.0000	16.0000	12.0000	2.0000	1.0000	3.0000	7.0000	16.0000	6.0000	21.0000	12.0000	21.0000	8.0000	4.0000	8.0000	16.0000	17.0000	16.0000	5.0000	5.0000
A	3.0000	2.0000	1.0000	2.0000	1.0000	3.0000	4.0000	1.0000	1.0000	1.0000	1.0000	7.0000	6.0000	2.0000	3.0000	3.0000	4.0000	8.0000	4.0000	1.0000
Ar	1.4640	1.0630	1.0000	1.6670	1.0000	1.7330	1.7580	1.0000	1.0000	1.0000	1.0000	1.5150	1.7170	1.4290	1.4920	1.4860	1.6080	1.6980	1.6440	1.0000
H _O	0.2500	0.0625	0.0000	0.0000	0.0000	0.6667	0.4286	0.0000	0.0000	0.0000	0.0000	0.4286	0.7500	0.0000	0.6250	0.4375	0.4118	0.3750	0.8000	0.0000
H _E	0.4063	0.0605	0.0000	0.5000	0.0000	0.6111	0.7041	0.0000	0.0000	0.0000	0.0000	0.5023	0.6719	0.3750	0.4609	0.4707	0.5900	0.6758	0.5800	0.0000
FIS	0.5000	0.0000	NA	1.0000	NA	0.1110	0.4550	NA	NA	NA	NA	0.1710	-0.0500	1.0000	-0.2960	0.1030	0.3290	0.4710	-0.2800	NA
NA	0.0009	0.0000	0.0010	0.3333	0.0010	0.0000	0.1616	0.0010	0.0010	0.0010	0.0010	0.0000	0.0000	0.2903	0.0000	0.0207	0.1165	0.1652	0.0000	0.0010
HWE	0.1445	-	-	0.3320	-	1.0000	0.1619	-	-	-	-	0.0344*	0.0229*	0.1429	1.0000	1.0000	0.1040	0.0000*	1.0000	-

Table II. Distribution of the COI haplotypes in the *Raja miraletus* population samples

Haplotype	SAMPLES																				
	SAC/06/07 N=10	SAC/11 N=30	ANC/06 N=27	SEC/07 N=5	POC/07 N=11	AGC/03 N=8	AGC/10 N=8	BIS/06 N=19	SDC/05 N=11	TUC/06 N=22	TUC/10 N=6	ADV/14 N=17	MAL/02 N=22	JON/04 N=3	FNC/04 N=30	FNC/07 N=25	PGC/04 N=16	ABC/04 N=14	GRE/14 N=14	ILC/09 N=2	TKC/09 N=11
Hap_1	0.6000	0.4670																			
Hap_2	0.2000	0.2000																			
Hap_3	0.1000	0.1670																			
Hap_4	0.1000	0.0000																			
Hap_5		0.0333																			
Hap_6		0.0333																			
Hap_7		0.0333																			
Hap_8		0.0333																			
Hap_9		0.0333																			
Hap_10			0.2590																		
Hap_11			0.0370																		
Hap_12			0.1480																		
Hap_13			0.0741																		
Hap_14			0.0741																		
Hap_15			0.0370																		
Hap_16			0.2590																		
Hap_17			0.0370																		
Hap_18			0.0370																		
Hap_19			0.0370																		
Hap_20				0.6000																	
Hap_21				0.2000																	
Hap_22				0.2000																	
Hap_23					1.0000	1.0000	0.5000					0.2730	0.1180								
Hap_24							0.2500	1.0000	1.0000	0.9550	1.0000	0.2270	0.2940		0.3330	0.2800	0.0625	0.2140			
Hap_25							0.1250														
Hap_26							0.1250							0.3530	1.0000						
Hap_27										0.0455											
Hap_28														0.1180							
Hap_29														0.0588							
Hap_30														0.0588							
Hap_31																				1.0000	0.0000
Hap_32															0.5670	0.7200	0.8750	0.7860			
Hap_33															0.0333						
Hap_34															0.0333						
Hap_35																	0.0625				
Hap_36																			0.5710		
Hap_37																			0.4290		
Hap_38																					1.0000

